Markovian modeling of classical thermal noise in two inductively coupled wire loops

Daniel T. Gillespie*
Research and Technology Division, Naval Air Warfare Center, China Lake, California 93555
(Received 13 June 1996)

Continuous Markov process theory is used to model classical thermal noise in two wire loops of resistances R_1 and R_2, self-inductances L_1 and L_2, and absolute temperature T, which are coupled through their mutual inductance M. It is shown that even though the currents $I_1(t)$ and $I_2(t)$ in the two loops become progressively noisier as M increases from 0 toward its upper bound $(L_1L_2)^{1/2}$, the fluctuation-dissipation, Nyquist, and conductance formulas all remain unchanged. But changes do occur in the spectral density functions of the currents $I_i(t)$. Exact formulas for those functions are developed, and two special cases are examined in detail. (i) In the identical loop case ($R_1=R_2=R$ and $L_1=L_2=L$), the $M=0$ ''knee'' at frequency $R/2\pi L$ in the spectral density function of $I_i(t)$, below which that function has slope 0 and above which it has slope -2, is found to split when $M>0$ into two knees at frequencies $R/[2\pi(L\pm M)]$. The noise remains white, but surprisingly slightly suppressed, at frequencies below $R/[2\pi(L+M)]$, and it remains $1/f^2$ at frequencies above $R/[2\pi(L-M)]$. In between the two knee frequencies a rough ''$1/f$-type'' noise behavior is exhibited. The sum and difference currents $I_\pm(t)\equiv I_1(t)\pm I_2(t)$ are found to behave like thermal currents in two uncoupled loops with resistances R, self-inductances $(L\pm M)$, and temperatures $2T$. In the limit $M\to L$, $I_+(t)$ approaches the thermal current in a loop of resistance $\frac{1}{2}R$ and self-inductance L at temperature T, while $I_-(t)$ approaches $(4kT/R)^{1/2}$ times Gaussian white noise. (ii) In the weakly coupled highly dissimilar loop case ($R_1\ll R_2$, $L_1=L_2=L$, and $M\ll L$), $I_2(t)$ is found, to a first approximation, not to be affected by the presence of loop 1. But the spectral density function of $I_1(t)$ is found to be enhanced for frequencies $\nu\ll R_2/2\pi L$ by the approximate factor $(1+\alpha\nu^2)$, where $\alpha=(2\pi M)^2/R_1R_2$. A concomitant enhancement, by an approximate factor of $(1+2M^2R_2/L^2R_1)^{1/2}$, is found in the high-frequency amplitude noise of $I_1(t)$. An algorithm for numerically simulating $I_1(t)$ and $I_2(t)$ that is exact for all parameter values is presented, and simulation results that clarify and corroborate the theoretical findings are exhibited. [S1063-651X(97)15103-0]

PACS number(s): 05.40.+j, 02.50.Ga, 02.70.Lq, 72.70.+m

I. INTRODUCTION

In this paper we seek to describe theoretically the effects of classical thermal noise in two rigid wire loops of resistances R_1 and R_2, self-inductances L_1 and L_2, and mutual inductance M, the two loops being in thermal equilibrium at absolute temperature T.

The practical motivation for this investigation stems from the well-known fact that thermal noise ultimately imposes limitations on the performance abilities of very sensitive electronic devices that are required to operate under nonsuperconducting conditions. For example, the components of a very densely integrated microcircuit are necessarily situated closely together, and their consequent high inductive coupling affords a broad avenue for the propagation of ambient thermal noise. The double-loop problem considered here offers a simple prototype for studying the effects of inductively coupled thermal noise.

A less obvious practical system whose thermal noise sensitivity might be illuminated by an investigation of the double-loop problem is a medical magnetic resonance imaging (MRI) machine. The detector coils of a medical MRI machine are typically placed very close to the human body being examined, and the random thermal motions of naturally occurring solvated ions in the human body, mainly Na^+ and Cl^-, will generate random electromagnetic signals that will augment the ambient thermal noise in the detector coils, thereby degrading their performance. The ideal prototype for this problem would of course be a single R-L loop placed over a beaker of salt water, and that problem is currently under study by this writer. But it turns out that a crude surrogate for the beaker of salt water is a second R-L loop that has a much greater R/L ratio than the first; hence, the solution of the loop-loop problem for the limiting case $R_2/L_2\gg R_1/L_1$ is expected to provide some helpful guideposts for the solution of the much more complicated loop-ion problem.

The double-loop problem is of course a generalization of the classic single-loop problem of a rigid wire loop of resistance R and self-inductance L in thermal equilibrium at absolute temperature T. That problem had its origins in the 1928 works of Johnson [1] and Nyquist [2]; it was analyzed in more mathematical depth in 1945 by Wang and Uhlenbeck [3], and it is nowadays a fairly standard textbook topic [4–7]. To collect some formulas that we shall need for later reference, we begin by briefly summarizing the single-loop results, using the terminology and notation of a recent tutorial review [7].

Denoting the current in the R-L loop at time t by $I(t)$, we begin with the assumption that the interactions between the conducting electrons and the thermally vibrating atomic lattice of the wire give rise to a *thermal emf* of the two-term form $-RI(t)+V(t)$. Here $V(t)$, called the *Johnson emf*, is assumed to be a zero-mean randomly fluctuating quantity

*FAX: (619) 939-1409. Electronic address: dtg@rattler. chinalake.navy.mil

that is statistically independent of $I(t')$ for all $t' \leq t$. The circuit equation therefore reads

$$-RI(t)+V(t)-L\,\frac{dI(t)}{dt}=0. \tag{1.1}$$

The further assumption that classical statistical thermodynamics holds, in the sense that $\langle \frac{1}{2}LI^2(t\to\infty)\rangle = \frac{1}{2}kT$, where k is Boltzmann's constant, then leads to the following specific results.

(i) $I(t)$ is a univariate continuous Markov process of the Ornstein-Uhlenbeck type, with relaxation time L/R and diffusion constant $2kTR/L^2$. Given the initial condition $I(t_0)=i_0$, and denoting by $\mathcal{N}(m,\sigma^2)$ the normal random variable with mean m and variance σ^2, the solution to the single-loop circuit equation (1.1) is

$$I(t)=\mathcal{N}\left(i_0 e^{-(R/L)(t-t_0)},\ \frac{kT}{L}\,(1-e^{-2(R/L)(t-t_0)})\right) \quad (t\geq t_0). \tag{1.2}$$

A numerical simulation of the loop current can be effected by repeated application of the updating formula

$$I(t+\Delta t)=I(t)e^{-(R/L)\Delta t}+\left[\frac{kT}{L}\,(1-e^{-2(R/L)\Delta t})\right]^{1/2} n, \tag{1.3}$$

where n is a sample value of $\mathcal{N}(0,1)$; this updating formula is exact for any $\Delta t>0$.

(ii) The Johnson emf $V(t)$ is given in terms of the temperature T and the resistance R by the fluctuation-dissipation formula,

$$V(t)=(2kTR)^{1/2}\Gamma(t). \tag{1.4}$$

Here $\Gamma(t)$ is *Gaussian white noise*, a temporally uncorrelated normal random variable with mean 0 and variance $\delta(0)$, where δ is the Dirac delta function. The spectral density function $S_V(\nu)$ of $V(t)$, defined so that $S_V(\nu)d\nu$ measures the amount of $\langle V^2(t)\rangle$ in the positive cycle frequency interval $[\nu,\nu+d\nu)$, is given by *Nyquist's formula*,

$$S_V(\nu)=4kTR \quad (\nu\geq 0). \tag{1.5}$$

(iii) The equilibrium loop current

$$I^*(t)\equiv \lim_{t_0\to-\infty} I(t)=N(0,kT/L) \tag{1.6}$$

has spectral density function

$$S_I(\nu)=\frac{4kT}{R}\left(\frac{1}{1+(2\pi L\nu/R)^2}\right) \quad (\nu\geq 0). \tag{1.7}$$

$S_I(\nu)d\nu$ measures the amount of $\langle I^{*2}(t)\rangle$ in the frequency interval $[\nu,\nu+d\nu)$. A log-log plot of $S_I(\nu)$ shows a ''knee'' at frequency $R/2\pi L$, below which the curve has slope 0 and above which it has slope -2.

(iv) And finally, the autocovariance of the equilibrium current, namely $\langle I^*(t_1)I^*(t_2)\rangle$, is related to the loop resistance R through the *conductance formula*,

$$R^{-1}=\frac{1}{kT}\int_0^\infty \langle I^*(t)I^*(t+t')\rangle dt'. \tag{1.8}$$

Our plan here is as follows. In Sec. II we shall write down the circuit equations for two inductively coupled loops, and then use bivariate continuous Markov process theory to solve those equations subject to the requisite thermodynamic boundary conditions; in particular, we shall derive exact general formulas for the spectral density functions of the loop currents, and also derive an exact updating formula for numerically simulating those currents. In Sec. III we shall examine the implications of these general results for the case of two identical loops. And in Sec. IV we shall consider the case of two very dissimilar loops with weak coupling, this being the study model for the previously mentioned loop-ion problem. A brief summary of all our principal findings is given in Sec. V.

II. THERMAL CURRENTS IN TWO INDUCTIVELY COUPLED WIRE LOOPS

A. The double-loop circuit equations

Our analysis of the currents $I_1(t)$ and $I_2(t)$ in the two loops begins with the usual hypothesis that the interactions between the conducting electrons and the thermally vibrating atomic lattice of wire loop i $(i=1,2)$ give rise to a *thermal emf* of the two-term form $-R_iI_i(t)+V_i(t)$, where $V_i(t)$ is assumed to be a temporally uncorrelated, zero-mean random variable that is independent of both $I_1(t)$ and $I_2(t)$. We call $R_iI_i(t)$ the *dissipative voltage* in loop i, and $V_i(t)$ the *Johnson emf* in loop i. The self- and mutual inductances are by definition such that the instantaneous magnetic fluxes $\Phi_1(t)$ and $\Phi_2(t)$ linking the respective loops are given by

$$\Phi_1(t)=L_1I_1(t)+MI_2(t) \quad \text{and} \quad \Phi_2(t)=L_2I_2(t)+MI_1(t). \tag{2.1}$$

According to Faraday's law, any temporal variation in $\Phi_i(t)$ will give rise to an emf $-d\Phi_i(t)/dt$ in loop i. The requirement that the integral of the electric potential around each loop must vanish therefore gives us the pair of relations

$$-R_iI_i(t)+V_i(t)-\frac{d\Phi_i(t)}{dt}=0 \quad (i=1,2). \tag{2.2}$$

Substituting Eqs. (2.1) into Eqs. (2.2) and then solving the resulting pair of equations simultaneously for $dI_1(t)/dt$ and $dI_2(t)/dt$, we obtain

$$\frac{dI_1(t)}{dt}=-\frac{L_2R_1}{\kappa}\,I_1(t)+\frac{MR_2}{\kappa}\,I_2(t)+\frac{L_2}{\kappa}\,V_1(t)-\frac{M}{\kappa}\,V_2(t), \tag{2.3a}$$

$$\frac{dI_2(t)}{dt}=\frac{MR_1}{\kappa}\,I_1(t)-\frac{L_1R_2}{\kappa}\,I_2(t)-\frac{M}{\kappa}\,V_1(t)+\frac{L_1}{\kappa}\,V_2(t), \tag{2.3b}$$

where we have introduced the parameter

$$\kappa\equiv L_1L_2-M^2. \tag{2.4}$$

Energy considerations can be shown [8] to require that $M^2<L_1L_2$, so κ is strictly positive.

Since the Johnson emf's $V_1(t)$ and $V_2(t)$ in Eqs. (2.3) are hypothesized to be independent of $I_1(t')$ and $I_2(t')$ for all $t'<t$, then Eqs. (2.3) evidently constitute a set of ''memoryless'' time-evolution equations for those currents; i.e., they imply that the future behavior of those currents depends on their past values only through their present values. It follows that the variables $I_1(t)$ and $I_2(t)$ constitute a *bivariate continuous Markov process*, and accordingly must satisfy a bivariate Langevin equation [3,5,6,9]. But Eqs. (2.3) will be of the canonical bivariate Langevin form if and only if $V_1(t)$ and $V_2(t)$, which have been assumed to be independent of $I_1(t')$ and $I_2(t')$ also for $t'=t$, have the mathematical forms

$$V_i(t)=a_i\Gamma_i(t) \quad (i=1,2). \tag{2.5}$$

Here, a_1 and a_2 are constants, and $\Gamma_1(t)$ and $\Gamma_2(t)$ are statistically independent Gaussian white noise processes. Only with such Gaussian white noise involvement will the memoryless time evolutions of $I_1(t)$ and $I_2(t)$ dictated by Eqs. (2.3) be self-consistent [9].

As regards the constants a_1 and a_2, we shall prove in Sec. II C that agreement with classical statistical thermodynamics will be obtained if and only if

$$a_i=(2kTR_i)^{1/2} \quad (i=1,2). \tag{2.6}$$

This is equivalent to the uncoupled $M=0$ result in Eq. (1.4). The plausibility of Eq. (2.6) for $M\neq 0$ may not be universally acknowledged, as some might maintain that the noise that is inductively fed into loop 1 from loop 2 acts to augment $V_1(t)$ and its spectral density function $S_1(\nu)$, and thereby augments even R_1 through the Nyquist formula (1.5). The arguments in Sec. II C that derive Eq. (2.6) will show that does not happen. But for now, we shall simply regard a_1 and a_2 as two constants whose values remain to be determined.

With Eqs. (2.5), the circuit equations (2.3) now assume the canonical bivariate ''white-noise'' Langevin form [3,5,6,9]:

$$\frac{dI_1(t)}{dt}=-\frac{L_2R_1}{\kappa}I_1(t)+\frac{MR_2}{\kappa}I_2(t)+\frac{L_2a_1}{\kappa}\Gamma_1(t)-\frac{Ma_2}{\kappa}\Gamma_2(t), \tag{2.7a}$$

$$\frac{dI_2(t)}{dt}=\frac{MR_1}{\kappa}I_1(t)-\frac{L_1R_2}{\kappa}I_2(t)-\frac{Ma_1}{\kappa}\Gamma_1(t)+\frac{L_1a_2}{\kappa}\Gamma_2(t). \tag{2.7b}$$

B. Solving the circuit equations

Equations (2.7) are of a type that can be solved exactly, but several solution methods exist. One way of proceeding is to write down the equivalent bivariate forward Fokker-Planck equation, and then solve that equation for the joint density function of $I_1(t)$ and $I_2(t)$; this is the approach taken by van Kampen [5] and Risken [10]. Another way of proceeding is to solve the stochastic differential equation (2.7) directly using the formal calculi of Ito or Stratonovich, as has been done by Gardiner [6] and Honerkamp [11]. All methods of solution yield mathematically equivalent results, but those results are rendered in different ways. The choice of a solution method depends to a large extent upon what one intends to do with the solution.

We shall use here a method of solution that is essentially equivalent to the Ito method, but which, being less encumbered with mathematical formalism, yields immediately computable results using familiar modes of mathematical reasoning. This approach is predicated on the fact, emphasized in Ref. [9], that the continuous, memoryless functions I_1 and I_2 defined by Eqs. (2.7) are not in fact differentiable, and that the real meaning of Eqs. (2.7) is that the processes I_1 and I_2 evolve in time according to the following ''infinitesimal updating'' formulas:

$$I_1(t+dt)=I_1(t)-\frac{L_2R_1}{\kappa}I_1(t)dt+\frac{MR_2}{\kappa}I_2(t)dt+\frac{L_2a_1}{\kappa}N_1(t)(dt)^{1/2}-\frac{Ma_2}{\kappa}N_2(t)(dt)^{1/2}, \tag{2.8a}$$

$$I_2(t+dt)=I_2(t)+\frac{MR_1}{\kappa}I_1(t)dt-\frac{L_1R_2}{\kappa}I_2(t)dt-\frac{Ma_1}{\kappa}N_1(t)(dt)^{1/2}+\frac{L_1a_2}{\kappa}N_2(t)(dt)^{1/2}. \tag{2.8b}$$

Here, dt is a *non-negative infinitesimal variable*, i.e., a real variable that is confined to some interval $[0,\varepsilon]$ where ε is some arbitrarily small positive number, and $N_1(t)$ and $N_2(t)$ are statistically independent, temporally uncorrelated normal random variables with means 0 and variances 1. We shall refer to Eqs. (2.8) as the ''standard-form'' bivariate Langevin equation. All subsequent results in this paper are derived from Eqs. (2.8); however, in the interest of brevity, we shall omit most of the computational details. We shall generally assume that Eqs. (2.8) are subject to the ''sure'' initial conditions

$$I_1(t_0)=i_{10} \quad \text{and} \quad I_2(t_0)=i_{20}. \tag{2.9}$$

The well established result [5,6,10,11] that $I_1(t)$ and $I_2(t)$ are *normal* for all $t>t_0$ is easily deduced from Eqs. (2.8) by appealing to the well-known theorem in random variable theory [12] that any linear combination of normal random variables, whether or not they are statistically independent, is also normal. Application of this theorem to Eqs. (2.8) for $t=t_0$ shows that $I_1(t_0+dt)$ and $I_2(t_0+dt)$ are both normal, and the result for all $t>t_0$ follows by induction.

Any pair of normal random variables is fully characterized by giving their two means, their two variances, and their covariance. Differential equations for these time-varying quantities can be obtained by algebraically manipulating Eqs. (2.8) and then averaging, using the facts that $\langle N_i(t)\rangle=0$, $\langle N_i^2(t)\rangle=1$, $\langle N_1(t)N_2(t)\rangle=0$, and $\langle I_i(t)N_j(t+t')\rangle=0$ for all $t'\geqslant 0$; these relations all follow

from the definition of $N_i(t)$. Thus, by averaging Eq. (2.8a) and then passing to the limit $dt \to 0$, we get

$$\frac{d}{dt}\langle I_1(t)\rangle = -\frac{L_2R_1}{\kappa}\langle I_1(t)\rangle + \frac{MR_2}{\kappa}\langle I_2(t)\rangle.$$

An analogous equation for $d\langle I_2(t)\rangle/dt$ follows from Eq. (2.8b). By averaging the square of Eq. (2.8a) and then passing to the limit $dt \to 0$, we get

$$\frac{d}{dt}\langle I_1^2(t)\rangle = -2\frac{L_2R_1}{\kappa}\langle I_1^2(t)\rangle + 2\frac{MR_2}{\kappa}\langle I_1(t)I_2(t)\rangle + \frac{L_2^2a_1^2 + M^2a_2^2}{\kappa^2}.$$

An analogous equation for $d\langle I_2^2(t)\rangle/dt$ follows from Eq. (2.8b). And by averaging the product of Eqs. (2.8a) and (2.8b) and then passing to the limit $dt \to 0$, we get

$$\frac{d}{dt}\langle I_1(t)I_2(t)\rangle = \frac{MR_1}{\kappa}\langle I_1^2(t)\rangle + \frac{MR_2}{\kappa}\langle I_2^2(t)\rangle - \frac{L_1R_2 + L_2R_1}{\kappa}\langle I_1(t)I_2(t)\rangle - \frac{M(L_1a_2^2 + L_2a_1^2)}{\kappa^2}.$$

Using these equations, it is straightforward to show that if we define the constants

$$\alpha_{11} = \kappa^{-1}L_2R_1, \quad \alpha_{12} = -\kappa^{-1}MR_2, \quad \alpha_{21} = -\kappa^{-1}MR_1, \quad \alpha_{22} = \kappa^{-1}L_1R_2, \tag{2.10}$$

and

$$b_1 = \kappa^{-2}(L_2^2a_1^2 + M^2a_2^2), \quad b_2 = -\kappa^{-2}M(L_1a_2^2 + L_2a_1^2), \quad b_3 = \kappa^{-2}(L_1^2a_2^2 + M^2a_1^2), \tag{2.11}$$

then the two means $m_i(t) \equiv \langle I_i(t)\rangle$ are the solutions of the differential equation

$$\frac{d}{dt}\begin{bmatrix} m_1(t) \\ m_2(t) \end{bmatrix} = -\begin{bmatrix} \alpha_{11} & \alpha_{12} \\ \alpha_{21} & \alpha_{22} \end{bmatrix}\begin{bmatrix} m_1(t) \\ m_2(t) \end{bmatrix}, \tag{2.12}$$

while the two variances $v_i(t) \equiv \langle I_i^2(t)\rangle - \langle I_i(t)\rangle^2$ and the covariance $c(t) \equiv \langle I_1(t)I_2(t)\rangle - \langle I_1(t)\rangle\langle I_2(t)\rangle$ are the solutions of the differential equation

$$\frac{d}{dt}\begin{bmatrix} v_1(t) \\ c(t) \\ v_2(t) \end{bmatrix} = -\begin{bmatrix} 2\alpha_{11} & 2\alpha_{12} & 0 \\ \alpha_{21} & (\alpha_{11}+\alpha_{22}) & \alpha_{12} \\ 0 & 2\alpha_{21} & 2\alpha_{22} \end{bmatrix}\begin{bmatrix} v_1(t) \\ c(t) \\ v_2(t) \end{bmatrix} + \begin{bmatrix} b_1 \\ b_2 \\ b_3 \end{bmatrix}. \tag{2.13}$$

Together with the *normality* of $I_1(t)$ and $I_2(t)$, the solution $[m_1(t), m_2(t)]^T$ to Eq. (2.12) for the initial condition $[m_1(0), m_2(0)]^T = [i_{10}, i_{20}]^T$, and the solution $[v_1(t), c(t), v_2(t)]^T$ to Eq. (2.13) for the initial conditions $[v_1(0), c(0), v_2(0)]^T = [0,0,0]^T$, provide a complete solution to Eqs. (2.7) or (2.8). A variety of formal renderings of that solution can be found in the literature [5,6,10,11], but none of these are especially convenient for our purposes here. We shall examine the asymptotic ($t - t_0 \to \infty$) solutions in Sec. II C, and develop full solutions in Sec. II E.

C. Thermodynamic, fluctuation-dissipation, and Nyquist relations

Now we shall establish that the results of the preceding subsection will be consistent with classical statistical thermodynamics if and only if the constants a_1 and a_2 have the values asserted in Eqs. (2.6). This will imply, because of Eqs. (2.5), that the Johnson emf's in the two loops are given by

$$V_i(t) = (2kTR_i)^{1/2}\Gamma_i(t) \quad (i = 1,2), \tag{2.14}$$

which is the standard single-loop fluctuation-dissipation formula (1.4). A well-known spectral analysis theorem [13] then implies that the spectral density function of $V_i(t)$ will be given by

$$S_{V_i}(\nu) = 4kTR_i \quad (\nu \geq 0; i = 1,2), \tag{2.15}$$

which is the standard single-loop Nyquist formula (1.5). The fact that the intrinsic Johnson noise formulas (2.14) and (2.15) do not involve M tells us that *the inductive coupling noise does not affect the intrinsic resistances of the loops*. This finding will be reinforced in Sec. II D.

The condition that $I_1(t)$ and $I_2(t)$ must behave, in the limit $t - t_0 \to \infty$, in accordance with classical statistical thermodynamics implies that $I_1(\infty)$ and $I_2(\infty)$ must be random variables with a Maxwell-Boltzmann distribution that is appropriate to the system temperature T. It follows that the average of any function h of $I_1(\infty)$ and $I_2(\infty)$ must be computable as

$$\langle h(I_1(\infty), I_2(\infty))\rangle = Z\int_{-\infty}^{\infty} di_1 \int_{-\infty}^{\infty} di_2 h(i_1,i_2) \times \exp\left(-\frac{E(i_1,i_2)}{kT}\right), \tag{2.16}$$

where k is Boltzmann's constant, $E(i_1,i_2)$ is the total energy of the system when the currents in the respective loops are equal to i_1 and i_2, and Z is such that $\langle 1\rangle = 1$. We shall assume that $E(i_1,i_2)$ is given by the usual classical electromagnetic formula [8],

$$E(i_1,i_2) = \tfrac{1}{2}L_1i_1^2 + \tfrac{1}{2}L_2i_2^2 + Mi_1i_2. \tag{2.17}$$

Some straightforward but slightly tedious computation will show that, for this energy formula, Eq. (2.16) gives

$$\langle I_1(\infty)\rangle = \langle I_2(\infty)\rangle = 0, \tag{2.18a}$$

$$\langle I_1^2(\infty)\rangle = \kappa^{-1}L_2kT, \quad \langle I_2^2(\infty)\rangle = \kappa^{-1}L_1kT, \tag{2.18b}$$

$$\langle I_1(\infty)I_2(\infty)\rangle = -\kappa^{-1}MkT. \tag{2.18c}$$

Equations (2.18) constitute a set of ''thermodynamic boundary conditions'' for the circuit equations (2.8). They also allow us to compute the average equilibrium energy of the system,

$$\langle E(I_1(\infty),I_2(\infty))\rangle = \tfrac{1}{2}L_1\langle I_1^2(\infty)\rangle + \tfrac{1}{2}L_2\langle I_2^2(\infty)\rangle + M\langle I_1(\infty)I_2(\infty)\rangle. \tag{2.19}$$

The conventional way of interpreting the three terms on the right here is to say that the first two terms represent the average energy ''in'' each loop, and the third term represents the average ''interaction'' energy between the loops. From Eqs. (2.18) it is easy to see that

$$\tfrac{1}{2}L_1\langle I_1^2(\infty)\rangle = \tfrac{1}{2}L_2\langle I_2^2(\infty)\rangle = \frac{kT}{2}\frac{L_1L_2}{L_1L_2-M^2}, \tag{2.20a}$$

$$M\langle I_1(\infty)I_2(\infty)\rangle = -kT\frac{M^2}{L_1L_2-M^2}. \tag{2.20b}$$

So if $M=0$, the equilibrium mean energy of each individual loop is $\frac{1}{2}kT$, and the equilibrium mean interaction energy is zero. As M is increased from 0 towards its maximum value $(L_1L_2)^{1/2}$, the mean energies of the individual loops increase in unison towards $+\infty$, while the mean interaction energy decreases toward $-\infty$. But summing the three energies in Eqs. (2.20) shows that the equilibrium mean *total* energy of the double-loop system is, for *any* value of M, always equal to kT, just as we should expect.

The thermodynamic relations (2.16) and (2.17) imply that $I_1(\infty)$ and $I_2(\infty)$ should be *normal*, and as noted in Sec. II B, that requirement is surely satisfied. It remains only to show that the differential equations (2.12) and (2.13) have asymptotic solutions that satisfy the thermodynamically required moment relations (2.18). The existence of finite, nonoscillatory $t\to\infty$ solutions to Eqs. (2.12) and (2.13) hinges on whether the square matrices in those equations have eigenvalues that are all *real* and *positive*. The eigenvalues λ_1 and λ_2 of the square matrix in the first moments equation (2.12) are the roots of its characteristic polynomial,

$$Q_m(\lambda) \equiv \begin{vmatrix} (\alpha_{11}-\lambda) & \alpha_{12} \\ \alpha_{21} & (\alpha_{22}-\lambda) \end{vmatrix} = \lambda^2 - \lambda\kappa^{-1}(L_1R_2+L_2R_1) + \kappa^{-1}R_1R_2, \tag{2.21}$$

where the second equality follows upon invoking the definitions (2.10) of the α_{ij}'s. Using the quadratic formula, we find that the eigenvalues λ_1 and λ_2 are given explicitly by

$$\lambda_{1/2} = \frac{(L_1R_2+L_2R_1) \mp [(L_1R_2+L_2R_1)^2 - 4\kappa R_1R_2]^{1/2}}{2\kappa}, \tag{2.22}$$

and it is not hard to show that these two eigenvalues are indeed always real and positive. The eigenvalues γ_1, γ_2, and γ_3 of the square matrix in the second moments equation (2.13) are the roots of its characteristic polynomial,

$$\begin{aligned} Q_v(\gamma) &\equiv \begin{vmatrix} (2\alpha_{11}-\gamma) & 2\alpha_{12} & 0 \\ \alpha_{21} & (\alpha_{11}+\alpha_{22}-\gamma) & \alpha_{12} \\ 0 & 2\alpha_{21} & (2\alpha_{22}-\gamma) \end{vmatrix} \\ &= -\gamma^3 + \gamma^2 3\kappa^{-1}(L_1R_2+L_2R_1) \\ &\quad - \gamma 2\kappa^{-1}[\kappa^{-1}(L_1R_2+L_2R_1)^2 + 2R_1R_2] \\ &\quad + 4\kappa^{-2}R_1R_2(L_1R_2+L_2R_1), \end{aligned} \tag{2.23}$$

where again the second equality follows from the definitions (2.10) of the α_{ij}'s. Since this polynomial is strictly positive for all $\gamma\leqslant 0$, and approaches $-\infty$ as $\gamma\to\infty$, then it has no negative roots and at least one positive root. That the other two roots will be real (and hence positive) can be verified numerically in any specific case.

Since all the eigenvalues of Eqs. (2.12) and (2.13) are real and positive, then those equations must have constant asymptotic solutions. Clearly those solutions must satisfy

$$\begin{bmatrix} \alpha_{11} & \alpha_{12} \\ \alpha_{21} & \alpha_{22} \end{bmatrix}\begin{bmatrix} m_1(\infty) \\ m_2(\infty) \end{bmatrix} = \begin{bmatrix} 0 \\ 0 \end{bmatrix} \tag{2.24}$$

and

$$\begin{bmatrix} 2\alpha_{11} & 2\alpha_{12} & 0 \\ \alpha_{21} & (\alpha_{11}+\alpha_{22}) & \alpha_{12} \\ 0 & 2\alpha_{21} & 2\alpha_{22} \end{bmatrix}\begin{bmatrix} v_1(\infty) \\ c(\infty) \\ v_2(\infty) \end{bmatrix} = \begin{bmatrix} b_1 \\ b_2 \\ b_3 \end{bmatrix}. \tag{2.25}$$

Consider first the pair of algebraic equations (2.24). Since the determinant of coefficients is $Q_m(0)=\kappa^{-1}R_1R_2>0$, then Cramer's rule implies that the only solutions are

$$m_1(\infty) = m_2(\infty) = 0. \tag{2.26}$$

So the thermodynamic requirements (2.18a) are satisfied. Given that fact, the remaining thermodynamic requirements (2.18b) and (2.18c) can be written simply as

$$v_1(\infty) = \frac{L_2kT}{\kappa}, \quad v_2(\infty) = \frac{L_1kT}{\kappa}, \quad c(\infty) = -\frac{MkT}{\kappa}. \tag{2.27}$$

Using the definitions (2.10) and (2.11), straightforward but rather tedious algebra reveals that the set of three coupled equations (2.25) has solutions (2.27) if and only if a_1 and a_2 have the values (2.6). We conclude that Eqs. (2.6) are a necessary and sufficient condition for our Markovian modeling to be consistent with classical thermodynamics. Henceforth, we shall regard a_i as simply an abbreviation for $(2kTR_i)^{1/2}$.

D. Spectral densities of the currents and the conductance formulas

We define the equilibrium loop currents $I_1^*(t)$ and $I_2^*(t)$ by

$$I_i^*(t) \equiv \lim_{t_0\to-\infty} I_i(t) \quad (i=1,2). \tag{2.28}$$

Since $I_i^*(t)$ is basically the same as $I_i(\infty)$, then the analysis in the preceding section shows that $I_i^*(t)$ is a stationary, zero-mean, normal random process whose variance is given

by the constant value $v_i(\infty)$ in Eqs. (2.27). It follows that $I_i^*(t)$ will have a spectral density function, $S_{I_i}(\nu)$, which is such that $S_{I_i}(\nu)d\nu$ gives the amount of $\langle I_i^{*2}(t)\rangle = v_i(\infty)$ due to frequencies in the positive infinitesimal interval $[\nu,\nu+d\nu)$. In this section we shall derive an explicit formula for $S_{I_1}(\nu)$; the companion formula for $S_{I_2}(\nu)$ will then follow by a simple $1\leftrightarrow 2$ interchange of all indices.

Denoting the autocovariance of $I_1^*(t)$ by

$$z_1(t') \equiv \langle I_1^*(t) I_1^*(t+t')\rangle \equiv \lim_{t_0 \to -\infty} \langle I_1(t) I_1(t+t')\rangle, \quad (2.29)$$

then according to elementary spectral theory [13], $S_{I_1}(\nu)$ can be computed as the positive-frequency Fourier amplitude of this autocovariance:

$$S_{I_1}(\nu) = 4\int_0^\infty z_1(t')\cos(2\pi\nu t')dt' \quad (\nu \geq 0). \quad (2.30)$$

To compute $z_1(t')$ for use in Eq. (2.30), we return to the two circuit equations (2.8). We first replace t by $t+t'$ and dt by dt'. Then, multiplying each of the resulting two equations through by $I_1(t)$ and averaging, we get

$$\begin{aligned}\langle I_1(t) I_1(t+t'+dt')\rangle &= \langle I_1(t) I_1(t+t')\rangle \\ &\quad - \kappa^{-1} L_2 R_1 \langle I_1(t) I_1(t+t')\rangle dt' \\ &\quad + \kappa^{-1} M R_2 \langle I_1(t) I_2(t+t')\rangle dt',\end{aligned}$$

$$\begin{aligned}\langle I_1(t) I_2(t+t'+dt')\rangle &= \langle I_1(t) I_2(t+t')\rangle \\ &\quad + \kappa^{-1} M R_1 \langle I_1(t) I_1(t+t')\rangle dt' \\ &\quad - \kappa^{-1} L_1 R_2 \langle I_1(t) I_2(t+t')\rangle dt'.\end{aligned}$$

Taking the limit $dt' \to 0$, and recalling the definitions (2.10), we obtain

$$\frac{d}{dt'}\begin{bmatrix}\langle I_1(t) I_1(t+t')\rangle \\ \langle I_1(t) I_2(t+t')\rangle\end{bmatrix} = -\begin{bmatrix}\alpha_{11} & \alpha_{12} \\ \alpha_{21} & \alpha_{22}\end{bmatrix}\begin{bmatrix}\langle I_1(t) I_1(t+t')\rangle \\ \langle I_1(t) I_2(t+t')\rangle\end{bmatrix}.$$

Finally, taking the limit $(t-t_0)\to\infty$ and introducing the auxiliary function

$$z_2(t') \equiv \langle I_1^*(t) I_2^*(t+t')\rangle \equiv \lim_{t_0 \to -\infty} \langle I_1(t) I_2(t+t')\rangle, \quad (2.31)$$

we get

$$\frac{d}{dt'}\begin{bmatrix}z_1(t') \\ z_2(t')\end{bmatrix} = -\begin{bmatrix}\alpha_{11} & \alpha_{12} \\ \alpha_{21} & \alpha_{22}\end{bmatrix}\begin{bmatrix}z_1(t') \\ z_2(t')\end{bmatrix}. \quad (2.32)$$

We shall compute $z_1(t')$ for Eq. (2.30) by solving Eqs. (3.32) subject to the initial conditions

$$z_1(0) = \kappa^{-1} L_2 kT, \quad z_2(0) = -\kappa^{-1} M kT, \quad (2.33)$$

which follow immediately from Eqs. (2.29), (2.31), and (2.27).

The eigenvalues λ_1 and λ_2 of the square matrix in Eq. (2.32) are given in Eq. (2.22). Those eigenvalues are *real*, *positive*, and in the $M \neq 0$ case of interest here, *distinct*. By appealing to the generic solution for a vector differential equation of this form [14], we ultimately find that

$$z_1(t') = s_1 e^{-\lambda_1 t'} + s_2 e^{-\lambda_2 t'} \quad (t' \geq 0), \quad (2.34)$$

where s_1 and s_2 are defined by

$$s_1 \equiv \frac{kT}{\kappa}\frac{L_2 + M\eta}{1 + (R_1/R_2)\eta^2}, \quad (2.35a)$$

$$s_2 \equiv \frac{L_2 kT}{\kappa} - s_1, \quad (2.35b)$$

with

$$\eta \equiv \frac{(L_1R_2 - L_2R_1) - [(L_1R_2 - L_2R_1)^2 + 4M^2R_1R_2]^{1/2}}{2MR_1}. \quad (2.36)$$

Substituting Eq. (2.34) into Eq. (2.30) and then performing the straightforward integration over t', we obtain the following formula for the spectral density function of $I_1^*(t)$:

$$S_{I_1}(\nu) = 4\left[\frac{s_1/\lambda_1}{1 + (2\pi\nu/\lambda_1)^2} + \frac{s_2/\lambda_2}{1 + (2\pi\nu/\lambda_2)^2}\right] \quad (\nu \geq 0). \quad (2.37)$$

Again, λ_1 and λ_2 are as given in Eq. (2.22), and s_1 and s_2 are given by Eqs. (2.35) and (2.36). As a rudimentary check on this result, one can easily verify, using Eqs. (2.35b) and (2.18b), that the integral of Eq. (2.37) over all $\nu > 0$ yields the required equilibrium current intensity $\langle I_1^2(\infty)\rangle$.

We shall examine the implications of Eq. (2.37) in detail for two special cases in Secs. III and IV. But two general results should be noted now. Both of these results derive from the fact that the integral of the intermediate formula (2.34) over all $t' > 0$ gives [15]

$$\int_0^\infty z_1(t')dt' = \frac{s_1}{\lambda_1} + \frac{s_2}{\lambda_2} = \frac{kT}{R_1}. \quad (2.38)$$

First, by setting $\nu = 0$ in Eq. (2.37) and then invoking the last part of Eq. (2.38), we see that $S_{I_1}(\nu = 0) = 4kT/R_1$, independently of M; therefore, *there is no inductive augmentation of the noise in the loop current near* $\nu = 0$.

Second, if we simply combine Eq. (2.38) with the definition of $z_1(t')$ in Eq. (2.29), we get

$$R_1^{-1} = \frac{1}{kT}\int_0^\infty \langle I_1^*(t) I_1^*(t+t')\rangle dt'. \quad (2.39)$$

This is the standard single-loop conductance formula (1.8). Its validity here tells us that, even though the behavior of the current in loop 1 is substantially altered by the presence of loop 2, the specific property of that current that characterizes the *resistance* of loop 1 is *not* altered. This finding provides additional support for the inference drawn earlier, in connection with Eqs. (2.14) and (2.15), that the noise transmitted between the two loops through their inductive coupling does not change the intrinsic resistances of the loops.

E. Monte Carlo simulation of the currents

The key to numerically simulating the currents in the loops lies in being able to compute, from the values of the currents at any time t, their values at any later time $t+\Delta t$. A simulation is then effected by starting with the initial current values (2.9) and repeatedly applying the ''updating algorithm'' to generate samplings of the currents at times $t_0+\Delta t$, $t_0+2\Delta t$, $t_0+3\Delta t$, etc. The simplest updating algorithm is the pair of formulas obtained by replacing, in the standard form Langevin equations (2.8), the *infinitesimal* variable dt by the *finite* variable Δt, but that updating algorithm will be accurate only if Δt is ''sufficiently small.'' We present now an updating algorithm that is practically as fast, yet is *exact* for *any* positive value of Δt.

Assuming that the values of $I_1(t)$ and $I_2(t)$ are *known*, then by our results in Sec. II B, $I_1(t+\Delta t)$ and $I_2(t+\Delta t)$ will be *normal* random variables, whose means $m_1(\Delta t)$ and $m_2(\Delta t)$ are the $t=\Delta t$ solutions to Eqs. (2.12) for the initial conditions $m_1(0)=I_1(t)$ and $m_2(0)=I_2(t)$, and whose variances $v_1(\Delta t)$ and $v_2(\Delta t)$ and covariance $c(\Delta t)$ are the $t=\Delta t$ solutions to Eqs. (2.13) for the initial conditions $v_1(0)=c(0)=v_2(0)=0$. If we know the values of those five moments, then a simple result in random variable theory on the representation of two arbitrarily correlated normal random variables [16] allows us to compute $I_1(t+\Delta t)$ and $I_2(t+\Delta t)$ as

$$I_1(t+\Delta t)=m_1(\Delta t)+v_1^{1/2}(\Delta t)n_1, \tag{2.40a}$$

$$I_2(t+\Delta t)=m_2(\Delta t)+\frac{c(\Delta t)}{v_1^{1/2}(\Delta t)}\,n_1 + \left(v_2(\Delta t)-\frac{c^2(\Delta t)}{v_1(\Delta t)}\right)^{1/2} n_2, \tag{2.40b}$$

where n_1 and n_2 are two statistically independent samples of the random variable $\mathcal{N}(0,1)$ [17].

To implement the foregoing updating procedure, we evidently need to compute explicit expressions for the $t=\Delta t$ solutions $m_i(\Delta t)$, $v_i(\Delta t)$, and $c(\Delta t)$ to Eqs. (2.12) and (2.13). This can be accomplished by straightforwardly implementing the generic solution formula for a first-order, linear, matrix differential equation [14]. The result is the following *exact simulation algorithm*.

Step 1. Specify values for the physical parameters R_1, L_1, R_2, L_2, M, and kT, taking care to ensure that $0<M<(L_1L_2)^{1/2}$. Specify the initial values i_{10} and i_{20} of the loop currents. And specify values for the time-step Δt and a stopping time t_{stop}.

Step 2. Evaluate *quantities that will not change* during the course of the simulation: Compute κ from Eq. (2.4), a_1 and a_2 from Eqs. (2.6), the α_{ij}'s from Eqs. (2.10), and the b_i's from Eqs. (2.11). Compute the eigenvalues λ_i and eigenvectors $[u_{i1},u_{i2}]^T$ $(i=1,2)$ of the square matrix in Eq. (2.12), and in preparation for computing the expansion coefficients $\{\xi_i\}$ of $\mathbf{m}(0)\equiv\mathbf{I}(t)$ in the eigenvectors $\{\mathbf{u}_i\}$, compute the quantities

$$\theta_{11}=u_{22}/u_0,\quad \theta_{12}=-u_{21}/u_0,\quad \theta_{21}=-u_{12}/u_0,\quad \theta_{22}=u_{11}/u_0, \tag{2.41a}$$

where

$$u_0\equiv u_{11}u_{22}-u_{12}u_{21}. \tag{2.41b}$$

Compute the eigenvalues γ_i and eigenvectors $[w_{i1},w_{i2},w_{i3}]^T$ $(i=1,2,3)$ of the square matrix in Eq. (2.13), and compute the expansion coefficients $\{\beta_i\}$ of $\mathbf{b}\equiv[b_1,b_2,b_3]^T$ in the eigenvectors $\{\mathbf{w}_i\}$ by numerically solving the three simultaneous algebraic equations

$$b_j=\sum_{i=1}^{3}\beta_i w_{ij}\quad (j=1,2,3). \tag{2.42}$$

Compute finally the auxiliary quantities [14]

$$\mu_{ij}\equiv e^{-\lambda_i\Delta t}u_{ij}\quad (i,j=1,2), \tag{2.43}$$

$$\nu_{ij}\equiv\beta_i\left(\frac{1-e^{-\gamma_i\Delta t}}{\gamma_i}\right)w_{ij}\quad (i,j=1,2,3), \tag{2.44}$$

$$v_1(\Delta t)=\sum_{i=1}^{3}\nu_{i1},\quad c(\Delta t)=\sum_{i=1}^{3}\nu_{i2},\quad v_2(\Delta t)=\sum_{i=1}^{3}\nu_{i3}, \tag{2.45}$$

and

$$A_1\equiv v_1^{1/2}(\Delta t),\quad A_2\equiv\frac{c(\Delta t)}{v_1^{1/2}(\Delta t)},\quad A_3\equiv\left(v_2(\Delta t)-\frac{c^2(\Delta t)}{v_1(\Delta t)}\right)^{1/2}. \tag{2.46}$$

Step 3. With I_1 and I_2 representing the values of the loop currents at the ''present'' time t, initialize these variables by setting $t=0$, $I_1=i_{10}$, and $I_2=i_{20}$.

Step 4. Begin the main loop of the simulation by plotting out the points (t,I_1) and (t,I_2).

Step 5. Increase t by Δt. Terminate the simulation if the new t exceeds t_{stop}.

Step 6. Generate two independent sample values n_1 and n_2 of the unit normal random variable $\mathcal{N}(0,1)$ [17].

Step 7. Update the loop currents by first computing

$$\xi_i=\theta_{i1}I_1+\theta_{i2}I_2\quad (i=1,2), \tag{2.47}$$

then computing [14]

$$m_i=\xi_1\mu_{1i}+\xi_2\mu_{2i}\quad (i=1,2), \tag{2.48}$$

and finally putting, in accordance with Eqs. (2.40),

$$I_1=m_1+A_1n_1, \tag{2.49a}$$

$$I_2=m_2+A_2n_1+A_3n_2. \tag{2.49b}$$

Step 8. Return to Step 4.

Although the preparatory computations in Step 2 are numerous and somewhat involved, the computations that must be carried out at each time step (in Steps 5–7) are few and relatively easy. So this exact simulation procedure will be fast. Its execution time will be quite comparable to that of the approximate first-order updating formulas obtained by finitizing dt in the standard-form Langevin equations (2.8).

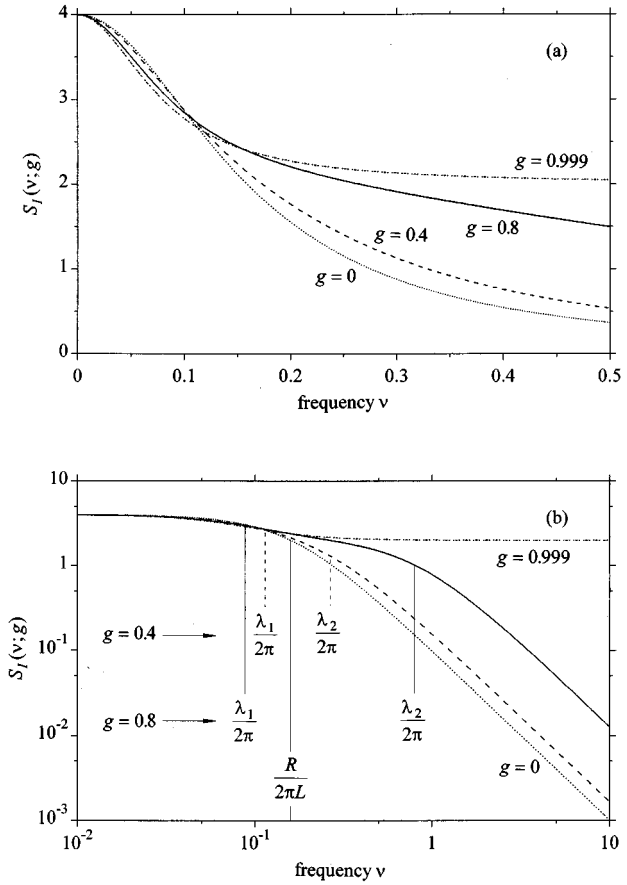

FIG. 1. Linear (a) and logarithmic (b) plots of $S_I(\nu;g)$ for the identical loop case with $R=L=kT=1$ and g values 0, 0.4, 0.8, and 0.999. In (a), note the slight noise *suppression* with increasing g at low frequencies. In (b), note how the knee frequency $R/2\pi L$ in the $g=0$ curve splits, for $g>0$, into two knees at frequencies $\lambda_1=L/2\pi R(1+g)$ and $\lambda_2=L/2\pi R(1-g)$, in between which a brief ''1/f-type'' noise behavior is exhibited.

Note that both updating algorithms require exactly two unit normal random numbers at each time step. Simulation results obtained using the exact algorithm will be exhibited for some specific cases in Secs. III and IV.

III. THE CASE OF IDENTICAL LOOPS

In this section we consider the identical loop case in which

$$R_1=R_2=R \quad \text{and} \quad L_1=L_2=L. \tag{3.1}$$

It will be convenient now to measure the inductive coupling between the two loops by

$$g\equiv M/L, \tag{3.2}$$

which evidently goes from 0 to 1 as the mutual inductance M goes from its lower limit 0 to its (unattainable) upper limit L. So $\kappa=L^2(1-g^2)$, and the asymptotic variances and covariance of the currents in the loops, as given in general by Eqs. (2.18), now read

$$\langle I_i^2(\infty)\rangle=\frac{kT}{L}\frac{1}{1-g^2} \quad (i=1,2), \tag{3.3a}$$

$$\langle I_1(\infty)I_2(\infty)\rangle=-\frac{kT}{L}\frac{g}{1-g^2}. \tag{3.3b}$$

These equations show that if g is increased from 0 towards 1, then the current in each loop becomes *increasingly noisy* and *increasingly anticorrelated*; indeed, the correlation coefficient of the loop currents can be seen from Eqs. (3.3) to be equal to $-g$, which approaches the fully anticorrelated value of -1 as g approaches its upper limit 1. In this section we shall examine some of the manifestations of these predicted behaviors.

A. Spectral density of the current

For the parameter values in Eqs. (3.1) and (3.2), we find that the eigenvalues λ_1 and λ_2 as given by Eqs. (2.22) become

$$\lambda_1=\frac{R}{L(1+g)} \quad \text{and} \quad \lambda_2=\frac{R}{L(1-g)}. \tag{3.4}$$

And upon chasing through the algebra of Eqs. (2.35) and (2.36), we find that formula (2.37) for the spectral density function of the asymptotic current in either loop becomes

$$S_I(\nu;g)=\frac{2kT}{R}\left(\frac{1}{1+[(2\pi L\nu/R)(1+g)]^2}+\frac{1}{1+[(2\pi L\nu/R)(1-g)]^2}\right), \tag{3.5}$$

where we now note explicitly the dependency of this function on the coupling constant g.

In Fig. 1 we show linear and logarithmic plots of $S_I(\nu;g)$ for $R=L=kT=1$ and g values 0, 0.4, 0.8, and 0.999. As can be seen in Fig. 1(b), the ''knee'' in the $g=0$ curve at frequency $R/2\pi L$ *splits*, for $g>0$, into *two* knees at frequencies $\lambda_1/2\pi$ and $\lambda_2/2\pi$. Below the lower knee frequency $\lambda_1/2\pi$ the logarithmic curve still has slope 0, and above the upper knee frequency $\lambda_2/2\pi$ it still has slope -2. But for frequencies lying between the two knee frequencies, the logarithmic curve is reasonably well approximated by a straight line whose slope is between 0 and -1. For example, in the logarithmic plot of $S_I(\nu,0.8)$ [the solid curve in Fig. 1(b)], the curve in the frequency decade between $\lambda_1/2\pi=1/2\pi(1+0.8)\approx 0.09$ and $\lambda_2/2\pi=1/2\pi(1-0.8)=0.8$ is found to be reasonably well approximated by a straight line of slope -0.35.

Some straightforward algebra leads to the following low-frequency and high-frequency approximations to Eq. (3.5):

$$S_I(\nu;g)\approx\begin{cases}\dfrac{4kT}{R}\left[1-\left(\dfrac{2\pi L}{R}\right)^2(1+g^2)\nu^2\right] & \text{for } \nu\ll\lambda_1/2\pi, \quad (3.6a)\\ \left(\dfrac{1+g^2}{(1-g^2)^2}\right)\dfrac{kTR}{\pi^2L^2}\dfrac{1}{\nu^2} & \text{for } \nu\gg\lambda_2/2\pi. \quad (3.6b)\end{cases}$$

Equation (3.6b) confirms the assertion that the high-frequency behavior of $S_I(\nu;g)$ is $1/f^2$. It also gives us, as the factor in parentheses on the right-hand side, the ''high-frequency enhancement ratio'' $S_I(\nu;g)/S_I(\nu;0)$. For $g\ll 1$ this ratio is quite small, being approximately equal to $1+3g^2$; however, the ratio evidently approaches ∞ as $g\to 1$. The ratio measures the high-frequency ''parallel displacements'' of the curves in Fig. 1(b) for successively higher g values. The consequent flattening out of the curve of $S_I(\nu;g)$ at large ν as $g\to 1$ is consistent with the divergence of the mean loop energy in that limit implied by Eq. (3.3a).

Equation (3.6a) shows that $S_I(0;g)$ is independent of g; thus, the inductive coupling has no effect on the noise level in the loop at $\nu=0$. But a very intriguing effect is indicated by Eq. (3.6a) at frequencies *just above* 0. There, larger values of g evidently *diminish* the noise in the loop. This ''low-frequency quieting'' can be seen most clearly in the linear plots of Fig. 1(a). It is a weak effect, but the fact that it occurs at all is very surprising. By simply bringing the two loops closer together, and thereby increasing g and the *total* noise in each loop, we will actually *reduce* the noise in each loop over a restricted range of low frequencies.

B. The sum and difference currents

In the identical loop case, the sum and difference currents,

$$I_\pm(t)\equiv I_1(t)\pm I_2(t), \quad (3.7)$$

exhibit a very interesting behavior. By substituting the identical loop parameters (3.1) and (3.2) into the general circuit equations (2)–(7), invoking the definitions of κ and a_i in Eqs. (2.4) and (2.6), and then computing the sum and difference of the resulting two equations, we get

$$\frac{dI_\pm(t)}{dt}=-\frac{R}{L(1\pm g)}I_\pm(t)+\frac{(2kTR)^{1/2}}{L(1\pm g)}[\Gamma_1(t)\pm\Gamma_2(t)]. \quad (3.8)$$

Since $\Gamma_1(t)$ and $\Gamma_2(t)$ are statistically independent normal random variables with means 0 and variances $\delta(0)$, then $\Gamma_1(t)\pm\Gamma_2(t)$ will be zero-mean normals with means 0 and variances $2\delta(0)$, which is the same as $\sqrt{2}$ times a zero-mean normal with mean 0 and variance $\delta(0)$ [18]; thus,

$$\Gamma_1(t)\pm\Gamma_2(t)=2^{1/2}\Gamma_\pm(t), \quad (3.9)$$

where $\Gamma_+(t)$ and $\Gamma_-(t)$ are Gaussian white noise processes. $\Gamma_+(t)$ and $\Gamma_-(t)$ are, moreover, *statistically independent* of each other; because, as can easily be shown from Eq. (3.9), $\langle\Gamma_+(t)\Gamma_-(t)\rangle=0$, and a vanishing covariance implies statistical independence for *normal* random variables. Substituting Eqs. (3.9) into Eqs. (3.8), we finally obtain

$$\frac{dI_\pm(t)}{dt}=-\frac{R}{L(1\pm g)}I_\pm(t)+\frac{[2k(2T)R]^{1/2}}{L(1\pm g)}\Gamma_\pm(t). \quad (3.10)$$

Equations (3.10) are interesting for several reasons. First, by comparing them with the canonical white noise form Ornstein-Uhlenbeck (OU) Langevin equation [19], we may deduce that $I_+(t)$ and $I_-(t)$ are OU processes with respective relaxation times and diffusion constants

$$\tau_\pm=\frac{L(1\pm g)}{R} \quad \text{and} \quad c_\pm=\frac{4kTR}{[L(1\pm g)]^2}. \quad (3.11)$$

Furthermore, $I_+(t)$ and $I_-(t)$ are *statistically independent* of each other, since their driving Gaussian white noise processes $\Gamma_+(t)$ and $\Gamma_-(t)$ are statistically independent. All this is rather remarkable since $I_+(t)$ and $I_-(t)$ are defined in terms of two processes, $I_1(t)$ and $I_2(t)$, that are themselves *not* individually Markovian and *not* statistically independent of each other. Since $\tau_-<\tau_+$, then we may expect $I_-(t)$ to be a ''faster moving'' process than $I_+(t)$. And recalling that an OU process with relaxation time τ and diffusion constant c is asymptotically $\mathcal{N}(0,c\tau/2)$ [19], we may infer from Eqs. (3.11) that

$$I_\pm(t\to\infty)=N\left(0,\frac{2kT}{L(1\pm g)}\right). \quad (3.12)$$

This shows that the asymptotic variance of $I_-(t)$ will be larger than that of $I_+(t)$, so we may expect $I_-(t)$ to be a more ''widely ranging'' process than $I_+(t)$.

A second interesting feature of Eqs. (3.10) emerges when we recall, from Eqs. (1.1) and (1.4), that the equation for the thermal current $I(t)$ in a wire loop of resistance R and self-inductance L at absolute temperature T is

$$\frac{dI(t)}{dt}=-\frac{R}{L}I(t)+\frac{(2kTR)^{1/2}}{L}\Gamma(t), \quad (3.13)$$

where $\Gamma(t)$ is Gaussian white noise. Comparing Eqs. (3.10) with Eq. (3.13), we see that $I_+(t)$ and $I_-(t)$ can be viewed as thermal currents in two *isolated* wire loops that have the following respective physical parameters:

$$R_\pm=R, \quad L_\pm=L(1\pm g), \quad T_\pm=2T. \quad (3.14)$$

Finally, it is interesting to examine what happens to the sum and difference currents in the limit that the coupling constant g approaches its upper limit 1. We can think of this limit being realized physically by bringing the two loops together so that they coalesce into a single loop. In the case of $I_+(t)$, the limit $g\to 1$ would seem to imply, from Eqs. (3.14), that $I_+(t)$ would become the thermal current in a loop with resistance R, self-inductance $2L$, and temperature

$2T$, but another interpretation is possible: If we put $g=1$ in the ''+'' version of Eq. (3.10), then we see that the result can be written as Eq. (3.13) with R replaced by $R/2$; hence, $I_+(t)$ becomes in the limit $g\to 1$ the thermal current in a wire loop of resistance $R/2$, self-inductance L, and absolute temperature T. This is physically quite reasonable. A merger of two identical loops should produce a loop with the *same* self-inductance and temperature, but *half* the resistance. And clearly, the total current in the resultant loop should be the *sum* of the currents in the two loops being merged. According to Eq. (3.12), $I_+(t)$ will have, in the limit $g\to 1$, an asymptotic variance of kT/L; that is the *same* as the asymptotic variances of $I_1(t)$ and $I_2(t)$ when they are uncoupled ($g=0$). But the ''+'' version of Eqs. (3.11) shows that the relaxation time of $I_+(t)$ will then be $2L/R$, which is *twice* that of $I_1(t)$ and $I_2(t)$ when they are uncoupled; so, although $I_+(t)$ will fluctuate over the same range as the uncoupled $I_1(t)$ and $I_2(t)$, it will do so at just half the speed.

To deduce the behavior of the difference current $I_-(t)$ in the limit $g\to 1$, we observe from the ''−'' version of Eqs. (3.11) that, in this limit, $\tau_-\to 0$ and $c_-\to\infty$ but

$$\tau_- c_-^{1/2}=\frac{L(1-g)}{R}\,\frac{(4kTR)^{1/2}}{L(1-g)}=\left(\frac{4kT}{R}\right)^{1/2}$$

remains *constant*. We thus infer from the zero-tau limit theorem for OU processes [19] that

$$\lim_{g\to 1} I_-(t)=\left(\frac{4kT}{R}\right)^{1/2}\Gamma(t), \tag{3.15}$$

where $\Gamma(t)$ is Gaussian white noise. This in turn implies, by a well-known theorem of spectral analysis [13], that the spectral density function of $I_-(t)$ in the limit $g\to 1$ is

$$\lim_{g\to 1} S_{I_-}(\nu)=\frac{8kT}{R}=2S_I(\nu=0;g=0)\quad(\nu\geqslant 0), \tag{3.16}$$

where the last step follows from Eq. (3.5).

C. Simulation results

Figures 2–6 show results obtained by using the simulation algorithm of Sec. II E to simulate the loop currents in the identical loop case with $R=L=kT=1$ and g values of 10^{-6}, 0.4, 0.8, 0.95, and 0.999. For each of the five simulation runs we took $\Delta t=0.001$ and $t_{\text{stop}}=9.0$. As discussed in Sec. II E, all of these simulations are *exact*; in particular, no errors arise because Δt is not a true infinitesimal. In each run, the loop currents $I_1(t)$ and $I_2(t)$ were generated first, using the aforementioned algorithm, and then the sum and difference currents $I_+(t)$ and $I_-(t)$ were computed from Eqs. (3.7). The dotted horizontal lines in the plots of $I_1(t)$ and $I_2(t)$ indicate their asymptotic one-standard deviation envelopes $\pm[kT/L(1-g^2)]^{1/2}$, as predicted by Eqs. (3.3a). The dotted horizontal lines in the plots of $I_+(t)$ and $I_-(t)$ indicate their asymptotic one-standard deviation envelopes $\pm[2kT/L(1\pm g)]^{1/2}$, as predicted by Eqs. (3.12).

The plots in Fig. 2 for $g=10^{-6}$ show an essentially *uncoupled* pair of loops for which the $I_1(t)$ and $I_2(t)$ trajectories are statistically identical and statistically independent,

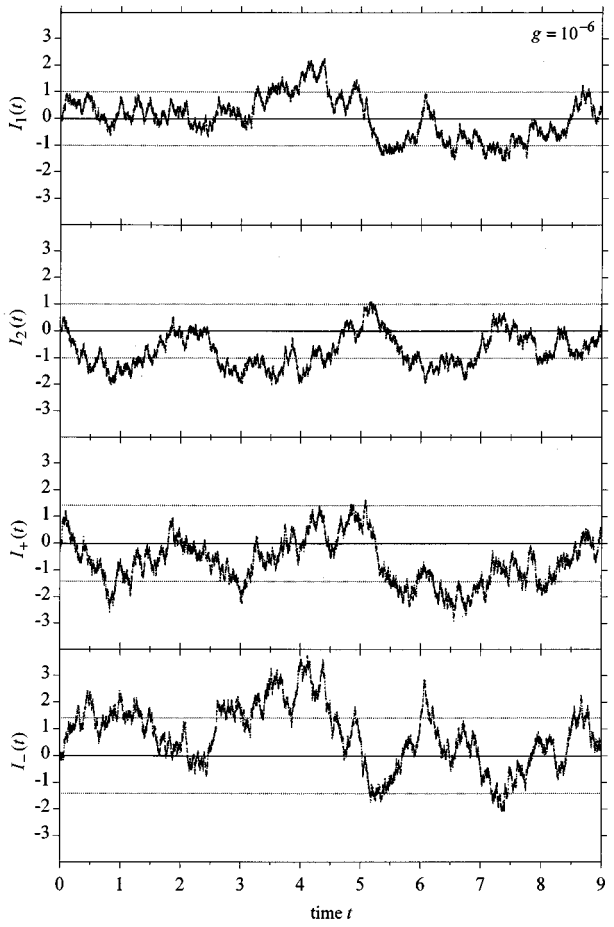

FIG. 2. Trajectories of $I_1(t)$, $I_2(t)$, $I_+(t)\equiv I_1(t)+I_2(t)$, and $I_-(t)\equiv I_1(t)-I_2(t)$, as computed using the exact simulation algorithm of Sec. II E for the identical loop case with $R=L=kT=1$, $g=10^{-6}$ (i.e., essentially zero coupling), $I_1(0)=I_2(0)=0$, and $\Delta t=0.001$. The dotted horizontal lines show the theoretically predicted asymptotic one-standard deviation envelopes. See the discussion in Sec. III C.

and likewise for the $I_+(t)$ and $I_-(t)$ trajectories. As g is steadily increased in the runs of Figs. 3–6, the $I_1(t)$ and $I_2(t)$ trajectories remain statistically identical but become increasing anticorrelated; by contrast, the $I_+(t)$ and $I_-(t)$ trajectories become statistically different and remain statistically independent. We have used the same base uniform random number sequence for all five runs in order to observe how various statistical idiosyncrasies in the trajectories change as g is increased. In the $I_1(t)$ and $I_2(t)$ trajectories, the fluctuations evidently become increasingly wild (note the vertical axis scale changes in Figs. 5 and 6), but at the same time those two trajectories become transformed into near mirror images of each other. At $g=0.999$, both $I_1(t)$ and $I_2(t)$ are giving fair imitations of white noise, as we should expect from their common spectral density curve in Fig. 1. The emerging *exact* Gaussian white noise behavior of $I_-(t)$, predicted by Eqs. (3.15) and (3.16), is evident in Fig. 6. But the companion $I_+(t)$ trajectory has evolved into a comparatively docile Ornstein-Uhlenbeck process, characterized, according to Eqs. (3.11), by the relaxation time $2L/R=2$ and the diffusion constant $kTR/L^2=1$. The difference between the ''texture'' of the $I_+(t)$ trajectory in Fig. 6 and the tex-

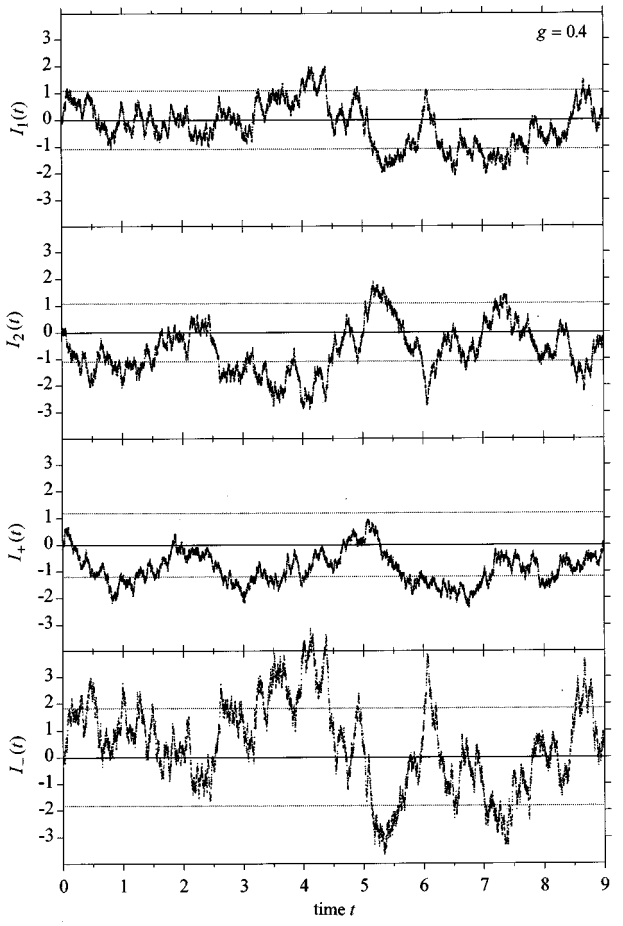

FIG. 3. As in Fig. 2, and using the same base random number sequence, except that $g=0.4$. See the discussion in Sec. III C.

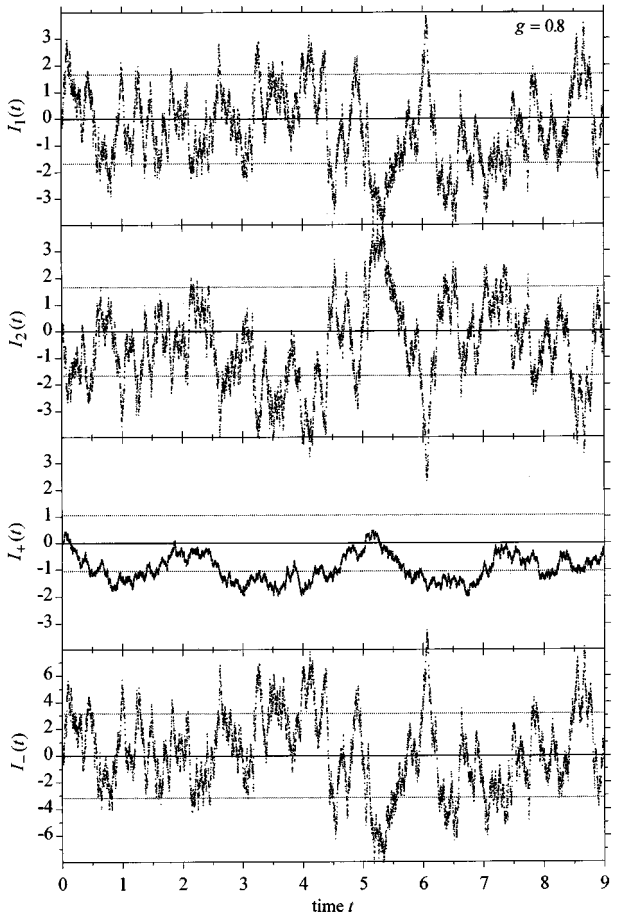

FIG. 4. As in Fig. 2, and using the same base random number sequence, except that $g=0.8$. See the discussion in Sec. III C.

tures of the $I_1(t)$ and $I_2(t)$ trajectories in Fig. 2 reflects the larger (by a factor of 2) relaxation time of $I_+(t)$.

IV. THE CASE OF VERY DISSIMILAR LOOPS WITH WEAK COUPLING

We now consider the case in which the resistance of loop 2 is very much larger than that of loop 1, while the inductive coupling between the two loops is very weak; specifically, we take

$$L_1=L_2=L, \tag{4.1a}$$

$$R_2\gg R_1, \tag{4.1b}$$

$$g\equiv M/L\ll 1. \tag{4.1c}$$

Since L_i/R_i measures the time scale of the intrinsic thermal fluctuations in loop i, then those fluctuations will be much more rapid in loop 2 than in loop 1. This problem serves as a highly simplified idealization of the problem in which loop 2 is replaced by a beaker of salt water, since the rapid fluctuations in loop 2 mimic the rapid Brownian movements of the Na^+ and Cl^- ions, which in turn induce a fluctuating emf in loop 1. The loop-ion problem will be addressed more directly in a later paper; however, one of our objectives here is to lay the foundation for some approximations that seem to be required to solve that more complicated problem.

Since the exact formula (2.37) for the spectral density function $S_{I_1}(\nu)$ of $I_1(t)$ is too complicated to analytically approximate according to Eqs. (4.1), we shall begin by using Eqs. (4.1) to analytically approximate the original circuit equations (2.8). Then we shall derive from the thus approximated circuit equations an approximate formula for $S_{I_1}(\nu)$. Finally, we shall numerically compare the predictions of that approximate formula with the predictions of the exact formula (2.37). We are interested here in not only the form and accuracy of the approximate solution, but also the logical thrust of the analysis that leads to it. We shall conclude by using the exact simulation algorithm of Sec. II E to see directly how the fluctuating character of the current in loop 1 is altered by the presence of loop 2.

A. The approximated circuit equations

With Eqs. (4.1a) and (4.1c), the definition of κ in Eq. (2.4) gives $\kappa\approx L^2$. Substituting this into the circuit equations (2.8) and again invoking Eq. (4.1a), we get

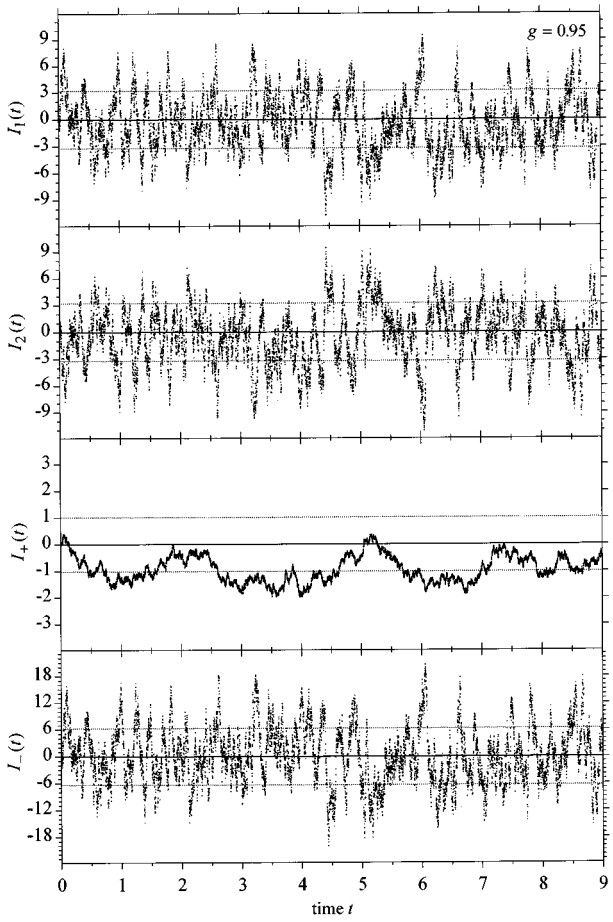

FIG. 5. As in Fig. 2, and using the same base random number sequence, except that $g=0.95$. See the discussion in Sec. III C.

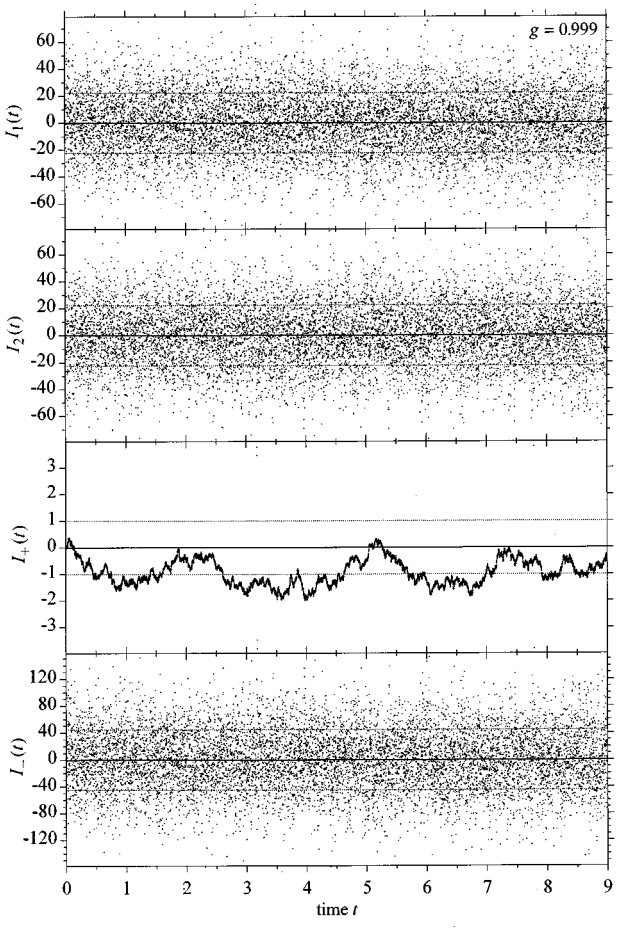

FIG. 6. As in Fig. 2, and using the same base random number sequence, except that $g=0.999$. See the discussion in Sec. III C.

$$I_1(t+dt)\approx I_1(t)-\frac{R_1}{L}\,I_1(t)dt+\frac{gR_2}{L}\,I_2(t)dt+\frac{a_1}{L}\,N_1(t)(dt)^{1/2}-\frac{ga_2}{L}\,N_2(t)(dt)^{1/2}, \tag{4.2a}$$

$$I_2(t+dt)\approx I_2(t)+\frac{gR_1}{L}\,I_1(t)dt-\frac{R_2}{L}\,I_2(t)dt-\frac{ga_1}{L}\,N_1(t)(dt)^{1/2}+\frac{a_2}{L}\,N_2(t)(dt)^{1/2}. \tag{4.2b}$$

Since $g\ll 1$ and $R_1\ll R_2$, then surely $gR_1\ll R_2$; therefore, inasmuch as $I_1(t)$ and $I_2(t)$ will typically have comparable magnitudes, by virtue of Eqs. (2.27), we may neglect on the right-hand side of Eq. (4.2b) the *second* term relative to the third term. Furthermore, since by Eq. (2.6) a_i is proportional $\sqrt{R_i}$, then surely $ga_1\ll a_2$; so, since $N_1(t)$ and $N_2(t)$ will typically have comparable magnitudes, we may also neglect on the right-hand side of Eq. (4.2b) the *fourth* term relative to the fifth term. We thus conclude that conditions (4.1) allow us to approximate Eqs. (2.8) by

$$I_1(t+dt)\approx I_1(t)-\frac{R_1}{L}\,I_1(t)dt+\frac{gR_2}{L}\,I_2(t)dt+\frac{a_1}{L}\,N_1(t)(dt)^{1/2}-\frac{ga_2}{L}\,N_2(t)(dt)^{1/2}, \tag{4.3a}$$

$$I_2(t+dt)\approx I_2(t)-\frac{R_2}{L}\,I_2(t)dt+\frac{a_2}{L}\,N_2(t)(dt)^{1/2}. \tag{4.3b}$$

Before we proceed to examine the implications of the approximate circuit equations (4.3), we want to take note of another way in which those equations might have been obtained. By using the definition of a_i and the fact that $N_i(t)(dt)^{1/2}=\Gamma_i(t)dt$, it is not hard to show that Eqs. (4.3) can be written equivalently as

$$-R_1I_1(t)+(2kTR_1)^{1/2}\Gamma_1(t)-\frac{d}{dt}\,[LI_1(t)+MI_2(t)]\approx 0, \tag{4.4a}$$

$$-R_2I_2(t)+(2kTR_2)^{1/2}\Gamma_2(t)-\frac{d}{dt}\,[LI_2(t)]\approx 0. \tag{4.4b}$$

These are evidently the circuit equations that we could have written down immediately *if* we had made the following two

assumptions: (i) the thermal emf's in the two loops are the same as they would be if the loops were isolated, and (ii) loop 2 does not see the Faraday emf produced by the current in loop 1. Assumption (i) is, as we saw in Sec. II C, strictly true, but assumption (ii) is an approximation that follows from conditions (4.1).

As can be seen from either Eqs. (4.3b) or (4.4b), $I_2(t)$ emerges in this approximation as the same *autonomous* process it would be if M were equal to zero; i.e., $I_2(t)$ is an Ornstein-Uhlenbeck process with relaxation time L/R_2 and diffusion constant $2kTR_2/L^2$.

To determine $I_1(t)$, we begin by squaring Eq. (4.3a), averaging the result, and then passing to the limit $dt\to 0$. Remembering that $a_i^2 = 2kTR_i$, we obtain

$$\frac{d}{dt}\langle I_1^2(t)\rangle \approx -2\frac{R_1}{L}\langle I_1^2(t)\rangle + 2\frac{gR_2}{L}\langle I_1(t)I_2(t)\rangle + \frac{2kT}{L^2}(R_1+g^2R_2). \tag{4.5a}$$

Performing these same operations on the product of Eqs. (4.3a) and (4.3b) gives

$$\frac{d}{dt}\langle I_1(t)I_2(t)\rangle \approx -\frac{(R_1+R_2)}{L}\langle I_1(t)I_2(t)\rangle + \frac{gR_2}{L}\langle I_2^2(t)\rangle - \frac{g2kTR_2}{L^2}. \tag{4.5b}$$

In the limit $t\to\infty$, the above two equations evidently become

$$0 \approx -2\frac{R_1}{L}\langle I_1^2(\infty)\rangle + 2\frac{gR_2}{L}\langle I_1(\infty)I_2(\infty)\rangle + \frac{2kT}{L^2}(R_1+g^2R_2), \tag{4.6a}$$

$$0 \approx -\frac{(R_1+R_2)}{L}\langle I_1(\infty)I_2(\infty)\rangle + \frac{gR_2}{L}\langle I_2^2(\infty)\rangle - \frac{g2kTR_2}{L^2}. \tag{4.6b}$$

Now, the approximate isolated character of $I_2(t)$ implies that $\langle I_2^2(\infty)\rangle \approx kT/L$. Inserting this into Eq. (4.6b) and then solving for $\langle I_1(\infty)I_2(\infty)\rangle$, we obtain

$$\langle I_1(\infty)I_2(\infty)\rangle \approx -\frac{gkT}{L(1+R_1/R_2)}. \tag{4.7}$$

And inserting this result into Eq. (4.6a) and then solving for $\langle I_1^2(\infty)\rangle$, we get

$$\langle I_1^2(\infty)\rangle \approx \frac{kT}{L}\left(1+\frac{g^2}{1+R_1/R_2}\right). \tag{4.8}$$

To check the results (4.7) and (4.8), which we shall make use of shortly, we note that the exact formulas (2.18) give, for $L_1 = L_2 = L$,

$$\langle I_1^2(\infty)\rangle = \frac{kT}{L(1-g^2)} \quad \text{and} \quad \langle I_1(\infty)I_2(\infty)\rangle = -\frac{gkT}{L(1-g^2)}.$$

Under our present restrictions $R_1 \ll R_2$ and $g \ll 1$, these exact results are indeed reasonably well approximated by Eqs. (4.7) and (4.8); in particular, we have from *either* $\langle I_1^2(\infty)\rangle$ formula that

$$\frac{L}{2}\langle I_1^2(\infty)\rangle \approx \frac{kT}{2}(1+g^2). \tag{4.9}$$

To compute the autocovariance $z_1(t')$ of the equilibrium current in loop 1, as defined in Eq. (2.29), we begin by replacing in Eqs. (4.3) t by $t+t'$ and dt by dt'. Then multiplying each of the resulting two equations through by $I_1(t)$ and averaging, we get

$$\langle I_1(t)I_1(t+t'+dt')\rangle \approx \langle I_1(t)I_1(t+t')\rangle - \frac{R_1}{L}\langle I_1(t)I_1(t+t')\rangle dt' + \frac{gR_2}{L}\langle I_1(t)I_2(t+t')\rangle dt',$$

$$\langle I_1(t)I_2(t+t'+dt')\rangle \approx \langle I_1(t)I_2(t+t')\rangle - \frac{R_2}{L}\langle I_1(t)I_2(t+t')\rangle dt'.$$

Now taking first the limit $dt'\to 0$, and then the limit $t_0\to-\infty$, we obtain, on account of the definitions (2.29) and (2.31),

$$\frac{d}{dt'}z_1(t') \approx -\frac{R_1}{L}z_1(t') + \frac{gR_2}{L}z_2(t'), \tag{4.10a}$$

$$\frac{d}{dt'}z_2(t') \approx -\frac{R_2}{L}z_2(t'). \tag{4.10b}$$

The definitions (2.29) and (2.31), along with our results (4.7) and (4.8), imply that the initial conditions for these two coupled differential equations are

$$z_1(0) = \langle I_1(\infty)I_1(\infty)\rangle \approx \frac{kT}{L}\left(1+\frac{g^2}{1+R_1/R_2}\right), \tag{4.11a}$$

$$z_2(0) = \langle I_1(\infty)I_2(\infty)\rangle \approx -\frac{gkT}{L(1+R_1/R_2)}. \tag{4.11b}$$

Equation (4.10b) is easily solved for $z_2(t')$ subject to the initial condition (4.11b). When that solution is substituted into Eq. (4.10a), one obtains a closed differential equation for $z_1(t')$ whose solution, for the initial condition (4.11a), is straightforwardly found to be

$$z_1(t') \approx \frac{kT}{L}\left\{\left(1-\frac{g^2(R_1/R_2)}{1-(R_1/R_2)^2}\right)e^{-(R_1/L)t'} + \frac{g^2}{1-(R_1/R_2)^2}e^{-(R_2/L)t'}\right\} \quad (R_2 \gg R_1, g \ll 1; t' \geq 0). \tag{4.12}$$

In the next section we shall see what this approximate formula for the autocovariance of the equilibrium current

$I_1^*(t)$ in loop 1 implies for the spectral density function of that current. As a check on Eq. (4.12), we note that by integrating it over all $t'>0$, we get

$$\int_0^\infty z_1(t')dt' \approx \frac{kT}{L}\left\{\left(1-\frac{g^2(R_1/R_2)}{1-(R_1/R_2)^2}\right)\frac{L}{R_1} + \frac{g^2}{1-(R_1/R_2)^2}\frac{L}{R_2}\right\} = \frac{kT}{R_1};$$

this, in light of the definition (2.29), is just the single-loop conductance formula (2.39).

B. Spectral densities of the currents

The approximate spectral density function of the equilibrium current in loop 2 under conditions (4.1) is of course the standard single-loop result (1.7) with $R=R_2$. To find the corresponding approximate spectral density function of the equilibrium current in loop 1, we must substitute our approximate formula (4.12) for $z_1(t')$ into Eq. (2.30) and then perform the t' integration. This is straightforwardly accomplished, and the result can be written in the form

$$S_{I_1}(\nu;g) \approx \frac{4kT}{R_1}\left(\frac{1}{1+(2\pi L\nu/R_1)^2}\right) \times\left[1+\frac{(2\pi Lg)^2}{R_1R_2}\frac{\nu^2}{1+(2\pi L\nu/R_2)^2}\right] \quad (R_2\gg R_1, g\ll 1; \nu\gtrsim 0). \quad (4.13)$$

A check on this result can be made by integrating it over all $\nu>0$; that yields precisely the estimate of $\langle I_1^2(\infty)\rangle$ in Eq. (4.8).

An inspection of Eq. (4.13) reveals that the factor in square brackets there is just the ratio of $S_{I_1}(\nu;g)$ to $S_{I_1}(\nu;0)$. For frequencies much less than $R_2/2\pi L$, which should be ''large'' since R_2 is presumed to be large, Eq. (4.13) implies that this *enhancement ratio* is given by

$$\frac{S_{I_1}(\nu;g)}{S_{I_1}(\nu;0)} \approx 1+\frac{(2\pi Lg)^2}{R_1R_2}\nu^2 \quad (R_2\gg R_1, g\ll 1; \nu\ll R_2/2\pi L). \quad (4.14)$$

Evidently, as ν increases from 0, the enhancement ratio increases from 1 in a *quadratic* fashion. But Eq. (4.13) shows that this quadratic increase with ν eventually levels off; specifically, Eq. (4.13) predicts that the enhancement ratio approaches the constant $1+g^2(R_2/R_1)$ as $\nu\to\infty$.

In Fig. 7(a) we show logarithmic plots of $S_{I_1}(\nu;g)$ versus ν for $L=R_1=kT=1$, $R_2=1000$, and g values of 0.1, 0.2, and 0.5. For each of these g values, we plot as a *solid* curve the *exact* spectral density function formula (2.37), and as a *dashed* curve the *approximate* spectral density function formula (4.13). For comparison, we have also shown the $g=0$ spectral density function as a dotted curve. The approximate formula is seen to work quite well for small g. For larger g it evidently underestimates the spectral density function at the higher frequencies; in particular, whereas Eq. (4.13) predicts, as just mentioned, a $\nu\to\infty$ enhancement ratio of

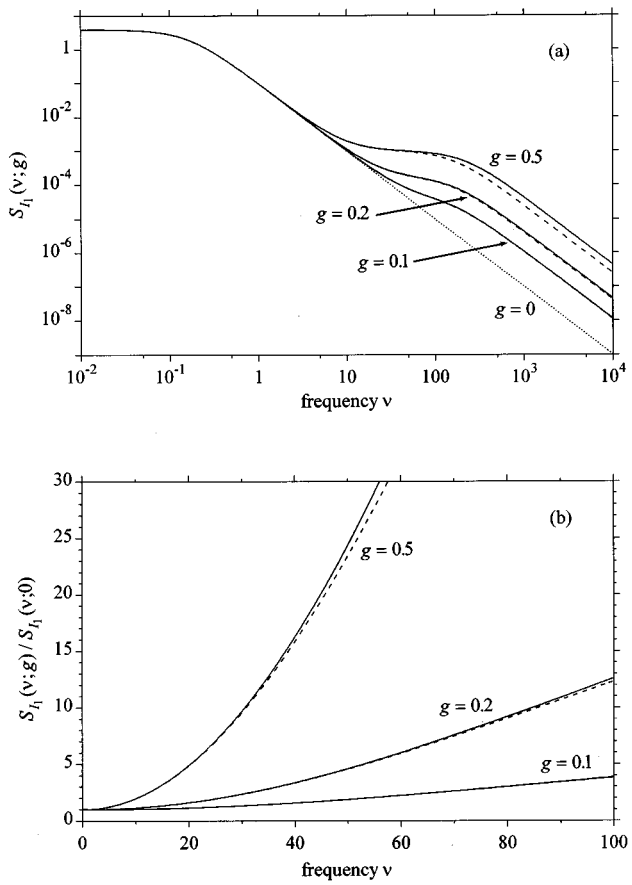

FIG. 7. Shown in (a) are logarithmic plots of $S_{I_1}(\nu;g)$ for $L_1=L_2=R_1=kT=1$, $R_2=1000$, and $g=0.1$, 0.2, 0.5, and also, for comparison, $g=0$ (as the dotted curve). In each of the $g>0$ cases, the solid curve shows the exact function (2.37) and the dashed curve shows the approximate function (4.13). Shown in (b) are linear plots of the ratio $S_{I_1}(\nu;g)/S_{I_1}(\nu;0)$ as computed from the exact formula (solid curve) and the approximate formula (dashed curve). The parabolic shapes for frequencies $\ll R_2/2\pi L\approx 159$ are the ''quadratic enhancement effect'' described by Eq. (4.14).

$$\lim_{\nu\to\infty}\frac{S_{I_1}(\nu;g)}{S_{I_1}(\nu;0)} \approx 1+g^2(R_2/R_1) \quad (R_2\gg R_1, g\ll 1), \quad (4.15a)$$

it turns out that an estimate of this ratio that is much more accurate for *any* g is

$$\lim_{\nu\to\infty}\frac{S_{I_1}(\nu;g)}{S_{I_1}(\nu;0)} \approx \frac{1}{1-g^2}\left(1+\frac{g^2(R_2/R_1)}{1-g^2}\right) \quad (R_2\gg R_1), \quad (4.15b)$$

which clearly *diverges* as $g\to 1$. The right side of Eq. (4.15a) gives the high-frequency upshifts of the *dashed* curves in Fig. 7(a), while the right side of Eq. (4.15b) describes very closely the high-frequency upshifts of the (exact) *solid* curves in Fig. 7(a). In Fig. 7(b) we plot, against linear axes, the ratio $S_{I_1}(\nu;g)/S_{I_1}(\nu;0)$ for the same g values examined in Fig. 7(a), again showing the predictions of the exact formula (2.37) as solid curves and the predictions of the approximate formula (4.13) as dashed curves. The parabolic

shapes of these curves at frequencies much less than $R_2/2\pi L \approx 159$ illustrates the ''quadratic frequency enhancement'' effect predicted by formula (4.14).

C. The enhanced Johnson noise

In this section we shall argue that, subject to some important caveats, we can *approximately* describe the effect on the current in loop 1 of the weakly coupled fast noise in loop 2 as a ''multiplicative enhancement'' of the high-frequency noise amplitude in loop 1.

We have seen that, under the conditions (4.1), the current in loop 2 behaves approximately as it would in the absence of loop 1; so $I_2(t)$ is approximately an Ornstein-Uhlenbeck process with relaxation time $\tau_2 = L/R_2$ and diffusion constant $c_2 = 2kTR_2/L^2$. Let us suppose that, as a result of satisfying condition (4.1b), R_2 is so large that the relaxation time τ_2 is *very small* on time scales of practical interest. Then, since $\tau_2 c_2^{1/2} = (2kT/R_2)^{1/2}$, we can invoke the zero-tau limit theorem for Ornstein-Uhlenbeck processes [19] to conclude that

$$I_2(t) \approx \left(\frac{2kT}{R_2}\right)^{1/2} \Gamma_2^*(t) \quad (g \ll 1,\ R_2\ \text{''large''}), \tag{4.16}$$

where $\Gamma_2^*(t)$ is a Gaussian white noise process. Substituting this approximation for $I_2(t)$ into the white noise version of the approximate circuit equation (4.3a) [which essentially replaces $N_i(t)(dt)^{1/2}$ with $\Gamma_i(t)dt$] and recalling the definition (2.6) of a_i, we get

$$\frac{d}{dt} I_1(t) \approx -\frac{R_1}{L} I_1(t) + \frac{(2kT)^{1/2}}{L} \times (gR_2^{1/2}\Gamma_2^*(t) + R_1^{1/2}\Gamma_1(t) - gR_2^{1/2}\Gamma_2(t)). \tag{4.17}$$

Since the Gaussian white noises $\Gamma_2^*(t)$, $\Gamma_1(t)$, and $\Gamma_2(t)$ are all statistically independent of each other [note that $\Gamma_2^*(t)$ is proportional to $I_2(t)$, which in turn is statistically independent of both $\Gamma_1(t)$ and $\Gamma_2(t)$], then the linear combination theorem for normal random variables allows us to write the last factor in Eq. (4.17) as

$$\begin{aligned} &gR_2^{1/2}\Gamma_2^*(t) + R_1^{1/2}\Gamma_1(t) - gR_2^{1/2}\Gamma_2(t) \\ &\quad = [g^2R_2 + R_1 + (-g)^2R_2]^{1/2}\Gamma_1^*(t) \\ &\quad = R_1^{1/2}(1 + 2g^2R_2/R_1)^{1/2}\Gamma_1^*(t), \end{aligned} \tag{4.18}$$

where $\Gamma_1^*(t)$ is yet another Gaussian white noise process. Substituting Eq. (4.18) into Eq. (4.17) gives us

$$\frac{d}{dt} I_1(t) \approx -\frac{R_1}{L} I_1(t) + \frac{(1 + 2g^2R_2/R_1)^{1/2}(2kTR_1)^{1/2}\Gamma_1^*(t)}{L}$$

$$(g \ll 1,\ R_2\ \text{''large''}). \tag{4.19}$$

We now observe that Eq. (4.19) is what we would write down as the circuit equation for loop 1 *if* we were told that it had resistance R_1, self-inductance L, and an *enhanced Johnson emf*

$$V_1^*(t) \equiv (1 + 2g^2R_2/R_1)^{1/2}(2kTR_1)^{1/2}\Gamma_1^*(t)$$

$$(g \ll 1,\ R_2\ \text{''large''}). \tag{4.20}$$

Comparing this with the formula (2.14) for the true Johnson emf $V_1(t)$ in loop 1, we see that the inductive coupling with loop 2 appears to have enhanced the Johnson emf in loop 1 by a factor of $(1+2g^2R_2/R_1)^{1/2}$. The expected effect of this enhancement can be inferred by multiplying Eq. (4.19) through by dt and examining the resultant formula for $I_1(t+dt) - I_1(t)$: one finds that *the very short time fluctuations in the current are augmented by a factor of* $(1+2g^2R_2/R_1)^{1/2}$.

But the foregoing conclusion must be qualified by several important caveats. First, as was noted below the exact formula (2.37) for $S_{I_1}(\nu)$, there is *never* any induced increase in the loop 1 noise at *zero* frequency. This can be seen quite clearly in the present case from the plots of $S_{I_1}(\nu)$ in Fig. 7(a), where the $g>0$ curves all lie on the $g=0$ curve at sufficiently low frequencies. It follows that the noise enhancement suggested by Eq. (4.20) can apply *only* to fluctuations with ''large'' frequencies or ''short'' periods.

Second, although Eq. (4.19) *appears* to have the form of the Ornstein-Uhlenbeck Langevin equation, which in turn would imply that $I_1(t)$ is a univariate continuous Markov process, this is emphatically *not* the case. The reason is that the white noise process $\Gamma_1^*(t)$ in Eq. (4.19) is *not* statistically independent of $I_1(t)$, as it would have to be if $I_1(t)$ were Markovian. One can verify this lack of statistical independence by directly computing the $t\to\infty$ average of the product of $I_1(t)$ and $\Gamma_1^*(t)$. Using Eqs. (4.18), (4.16), (4.7), and the fact that $I_1(t)$ is statistically independent of both $\Gamma_1(t)$ and $\Gamma_2(t)$, one can show that

$$\lim_{t\to\infty} \langle I_1(t)\Gamma_1^*(t)\rangle \approx -\frac{g^2R_2}{L(1+R_1/R_2)} \left(\frac{kT}{2(R_1+2g^2R_2)}\right)^{1/2}. \tag{4.21}$$

Evidently, this asymptotic covariance will not vanish, as statistical independency would require, unless g^2R_2 were effectively zero. But if g^2R_2 were effectively zero, then the enhancement term in formulas (4.19) and (4.20) would *also* be effectively zero. So Eq. (4.19) does *not* imply that $I_1(t)$ is *any* kind of univariate continuous Markov process.

The final important caveat concerning the enhanced Johnson noise formula (4.20) concerns writing that formula in the algebraically equivalent form

$$V_1^*(t) \equiv [2kT(R_1 + 2g^2R_2)]^{1/2}\Gamma_1^*(t)$$

$$(g \ll 1,\ R_2\ \text{''large''}). \tag{4.22}$$

This form might seem to suggest that the Johnson noise enhancement can be attributed to an enhancement in the resistance of loop 1 from R_1 to $R_1 + 2g^2R_2$. The fallacy of such a view can be seen in three different ways: First, the approximate circuit equation (4.19) *still* regards R_1 to be the loop resistance in the usual ''dissipative'' sense, inasmuch as the dissipative voltage still appears as $R_1 I_1(t)$. Second, it is clear from the generally valid conductance formula (2.39) that R_1^{-1} still plays the role of the true conductance of loop 1.

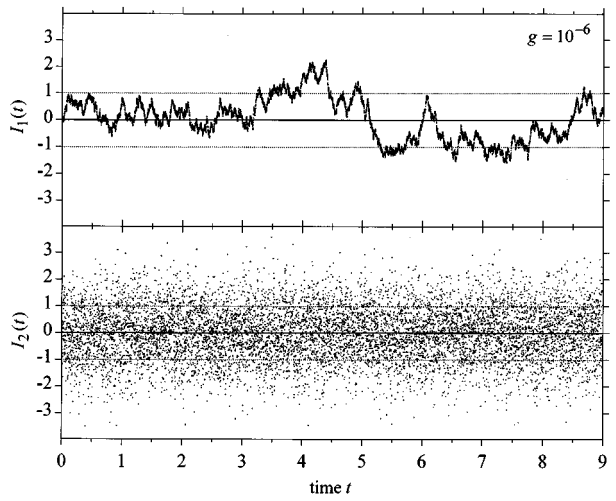

FIG. 8. Trajectories of $I_1(t)$ and $I_2(t)$, as computed using the exact simulation algorithm of Sec. II E, for the case $L_1=L_2=R_1=kT=1$, $R_2=1000$, $g=10^{-6}$ (i.e., essentially zero coupling), $I_1(0)=I_2(0)=0$, and $\Delta t=0.001$. The dotted horizontal lines show the theoretically predicted asymptotic one-standard deviation envelopes.

And finally, the approximate spectral density function (4.13) of the equilibrium current in loop 1 *cannot* be obtained from the $g=0$ formula (1.7) simply by writing the resistance in the latter formula as $R_1+2g^2R_2$; in particular, $S_{I_1}(\nu=0;g)$ should be independent of g.

In spite of these caveats, the exact simulation results presented next will show that the factor $(1+2g^2R_2/R_1)^{1/2}$ in Eq. (4.20) seems to provide a fairly reasonable estimate of the enhancement induced in the *high-frequency* noise in loop 1 under the conditions (4.1).

D. Simulation results

We show in Figs. 8 and 9 the results of some numerical simulations of the loop currents for the parameter values $L=kT=1$, $R_1=1$, $R_2=1000$, and several different g values. All of these simulations were carried out using the *exact* simulation algorithm described in Sec. II E.

Figure 8 shows $I_1(t)$ and $I_2(t)$ for the effectively uncoupled case $g=10^{-6}$ (cf. Fig. 2); here the two currents are essentially autonomous Ornstein-Uhlenbeck processes with the same asymptotic variances kT/L but very different relaxation times L/R_1 and L/R_2. Figures 9(a), 9(b), and 9(c) show $I_1(t)$ for three additional simulation runs, which were made using the same time step $\Delta t=0.001$ and the same uniform random number seed, but different g values of 0.1, 0.2, and 0.5. The companion trajectories of $I_2(t)$ are not shown because they look approximately the same as the one in Fig. 8, as we should expect from the approximate circuit equation (4.3b). [The asymptotic one-standard deviation envelopes of both $I_1(t)$ and $I_2(t)$ are actually observed in these exact simulations to be about 15% larger at $g=0.5$ than at $g=10^{-6}$, in accordance with the predictions of the exact formulas (2.18b).]

Let us examine the $I_1(t)$ trajectories in Figs. 8 and 9 in the light of the corresponding $S_{I_1}(\nu)$ curves in Fig. 7(a) and the following values (for $R_1=1$ and $R_2=1000$) of the approximate Johnson noise enhancement factor in formula (4.20):

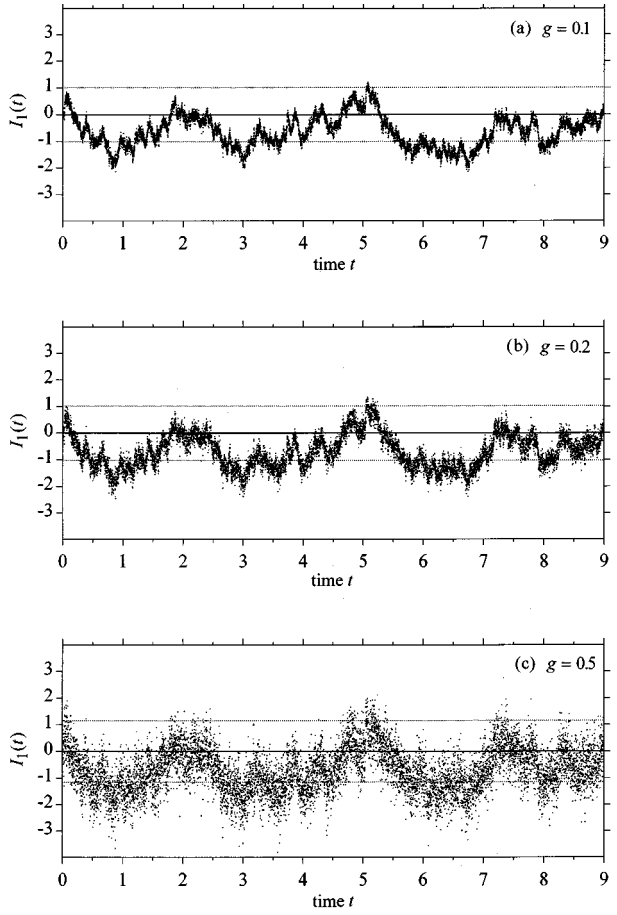

FIG. 9. Trajectories of $I_1(t)$, computed exactly as in Fig. 8 and with the same base random number sequence, but now with (a) $g=0.1$, (b) $g=0.2$, and (c) $g=0.5$. The companion $I_2(t)$ trajectories for these cases all look approximately the same as the one in Fig. 8. Subject to qualifications discussed in Sec. IV C, the high-frequency ''fuzzing'' of these trajectories is well described by the approximate ''thickening'' factor $(1+2g^2R_2/R_1)^{1/2}$.

g	$(1+2g^2R_2/R_1)^{1/2}$
0	1
0.1	4.6
0.2	9.0
0.5	22.4

According to the spectral density function plots in Fig. 7(a), not much inductive noise is introduced at frequencies below 2. And indeed, we see in the $I_1(t)$ trajectories in Fig. 9 that temporal fluctuations in $I_1(t)$ with periods greater than roughly 1/2 suffer little change with increasing g. But we can also see that, as g increases, the $I_1(t)$ trajectory gets increasingly ''fuzzed'' over shorter time intervals. And we observe that the consequent ''thickening'' of the trajectories is well described by the above values of the enhancement factor: The $g=0.1$ trajectory in Fig. 9(a) is roughly four times fatter than the $g\approx 0$ trajectory of $I_1(t)$ in Fig. 8; the $g=0.2$ trajectory in Fig. 9(b) is fatter again by a factor of roughly 2;

and the $g=0.5$ trajectory in Fig. 9(c) is fatter again by a factor of roughly 2 (even though this g value is no longer $\ll 1$).

V. SUMMARY AND CONCLUSIONS

We have used bivariate continuous Markov process theory to analyze the behavior of two wire loops of resistances R_1 and R_2, self-inductances L_1 and L_2, absolute temperature T, and mutual inductance M $(0 \leqslant M < [L_1 L_2]^{1/2})$. Our major assumptions were that classical statistical thermodynamics applies, and that the thermal noise in loop i $(i=1,2)$ can be described by a ''thermal emf'' of the form $-R_i I_i(t) + V_i(t)$, where $I_i(t)$ is the current in loop i and $V_i(t)$ is some zero-mean, temporally uncorrelated random process that is independent of $I_1(t)$ and $I_2(t)$.

We found that $I_1(t)$ and $I_2(t)$ must be normal random variables, whose means, variances, and covariance can be computed by solving the two matrix differential equations (2.12) and (2.13). The Johnson emf's $V_i(t)$ were shown to be unaffected by the inductive coupling between the loops, so the familiar single-loop fluctuation-dissipation and Nyquist formulas (2.14) and (2.15) remain valid. The single-loop conductance formula (2.39) was also shown to hold independently of M, thus implying that the noise introduced into each loop by the inductive coupling does not augment the effective resistances of the loops. An exact formula for the spectral density function of the equilibrium current in loop 1 was derived in Eq. (2.37), and an exact algorithm for numerically simulating the loop currents was presented in Sec. II E.

Two special cases were examined in detail. In the *identical loop case* $(R_1=R_2=R,\ L_1=L_2=L,\ g=M/L)$, the spectral density function of the loop current was found to be given by formula (3.5). As is shown in Fig. 1, the $M=0$ ''knee'' at frequency $R/2\pi L$, below which that function has slope 0 and above which it has slope -2, splits when $M>0$ into two knees at frequencies $R/2\pi(L \pm M)$. The noise remains white at frequencies below $R/2\pi(L+M)$, and $1/f^2$ at frequencies above $R/2\pi(L-M)$. In between the two knee frequencies a ''$1/f$-type'' noise behavior is briefly exhibited. A very slight but wholly unexpected *suppression* of the loop noise was found to occur at low frequencies [see Fig. 1(a) and Eq. (3.6a)]. The sum and difference currents $I_\pm(t) \equiv I_1(t) \pm I_2(t)$ were found to mimic the currents in two uncoupled loops with resistances R, self-inductances $(L \pm M)$, and temperatures $2T$. As $g \to 1$, $I_+(t)$ becomes the current in a loop of resistance $\frac{1}{2}R$ and self-inductance L at temperature T, while $I_-(t)$ approaches $(4kT/R)^{1/2}$ times Gaussian white noise. The increasingly wild, increasingly anticorrelated behavior of $I_1(t)$ and $I_2(t)$ with increasing g is shown clearly in the exact simulation plots of Figs. 2–6.

In the *weakly coupled highly dissimilar loop case* $(R_1 \ll R_2,\ L_1=L_2=L$, and $g \equiv M/L \ll 1)$, we found that $I_2(t)$ is not substantially affected by the presence of loop 1. This circumstance allowed an approximate analysis to be made, which revealed that the spectral density function of $I_1(t)$ is enhanced, for frequencies $\nu \ll R_2/2\pi L$, by the approximate factor $(1+\alpha\nu^2)$, where $\alpha = (2\pi L g)^2/R_1 R_2$. This *quadratic noise enhancement effect* is illustrated in Fig. 7(b). Also implied, and neatly verified by the exact simulations shown in Fig. 9, is an enhancement by a factor of $(1+2g^2 R_2/R_1)^{1/2}$ of the high-frequency amplitude noise in $I_1(t)$. This enhancement can be characterized roughly as an enhancement in the Johnson noise in loop 1, provided it is understood that there is no noise enhancement at low frequencies.

ACKNOWLEDGMENTS

The author thanks Carol Gillespie for computing and graphing all numerical data reported in this paper, and for making several helpful observations. This work was sponsored by the Inhouse Laboratory Independent Research Program of the Office of Naval Research.

[1] J. B. Johnson, Phys. Rev. **32**, 97 (1928).
[2] H. Nyquist, Phys. Rev. **32**, 110 (1928).
[3] Ming Chen Wang and G. E. Uhlenbeck, Rev. Mod. Phys. **17**, 323 (1945).
[4] F. Reif, *Fundamentals of Statistical and Thermal Physics* (McGraw-Hill, New York, 1965), Chap. 15.
[5] N. G. van Kampen, *Stochastic Processes in Physics and Chemistry* (North-Holland, Amsterdam, 1992).
[6] C. W. Gardiner, *Handbook of Stochastic Methods for Physics, Chemistry and the Natural Sciences* (Springer-Verlag, Berlin, 1985).
[7] D. T. Gillespie, Am. J. Phys. **64**, 225 (1996).
[8] See, for example, J. Reitz and F. Milford, *Foundations of Electromagnetic Theory* (Addison-Wesley, Reading, 1960), Chap. 12.
[9] D. T. Gillespie, Am. J. Phys. **64**, 1246 (1996).
[10] H. Risken, *The Fokker-Planck Equation* (Springer-Verlag, Berlin, 1984).
[11] J. Honerkamp, *Stochastic Dynamical Systems* (VCH, New York, 1994).
[12] See, for instance, M. D. Springer, *The Algebra of Random Variables* (Wiley, New York, 1979).
[13] See, for instance, Ref. [7], Sec. II E.
[14] If a constant $n \times n$ matrix A has a set of *real*, *positive*, and *distinct* eigenvalues $\{\lambda_i\}$, then its corresponding set of eigenvectors $\{\mathbf{v}_i\}$ will span n space, although not orthogonally if A is not symmetric (as it is not in our case). For such a matrix A, it is easy to prove that the solution of the differential equation $d\mathbf{x}(t)/dt = -A \cdot \mathbf{x}(t) + \mathbf{b}$, where $\mathbf{b}$ is a constant, can be written

$$\mathbf{x}(t) = \sum_{i=1}^{n} [\xi_{0i} e^{-\lambda_i (t-t_0)} + \beta_i \lambda_i^{-1} (1 - e^{-\lambda_i (t-t_0)})] \mathbf{v}_i ,$$

where ξ_{0i} and β_i are the expansion coefficients of $\mathbf{x}(t_0)$ and $\mathbf{b}$, respectively, in the set $\{\mathbf{v}_i\}$, i.e.,

$$\mathbf{x}(t_0) \equiv \sum_{i=1}^{n} \xi_{0i} \mathbf{v}_i , \quad \mathbf{b} \equiv \sum_{i=1}^{n} \beta_i \mathbf{v}_i .$$

Since the eigenvectors $\{\mathbf{v}_i\}$ in our case are not orthogonal, then the values $\{\xi_{0i}\}$ must be found by directly solving its defining set of n simultaneous linear equations, and likewise for the $\{\beta_i\}$.

[15] Although the *second* equality in Eq. (2.38) is in principle a purely algebraic consequence of Eqs. (2.22), (2.35), and (2.36), in practice the algebra borders on the intractable. There is a simpler way of establishing that second equality: Integrate Eq. (2.32) from $t'=0$ to ∞, using the fact that $z_1(\infty)=z_2(\infty)=0$ [see Eq. (2.34)], and get

$$-\begin{bmatrix} z_1(0) \\ z_2(0) \end{bmatrix} = -\begin{bmatrix} \alpha_{11} & \alpha_{12} \\ \alpha_{21} & \alpha_{22} \end{bmatrix} \begin{bmatrix} Z_1 \\ Z_2 \end{bmatrix},$$

where $Z_i=\int_0^\infty z_i(t')dt'$. Then, using the formulas for $z_i(0)$ and α_{ij} in Eqs. (2.33) and (2.10), a simple application of Cramer's rule yields $Z_1=kT/R_1$, which is the second part of Eqs. (2.38).

[16] D. T. Gillespie, Phys. Rev. E **54**, 2084 (1996), see Eqs. (3.2).

[17] An exact method for generating values for n_1 and n_2 is the so-called Box-Muller algorithm: Using two random numbers r_1 and r_2 uniform on [0,1], compute $s=[2\ln(1/r_1)]^{1/2}$ and $\theta=2\pi r_2$; then $n_1=s\cos\theta$ and $n_2=s\sin\theta$ will be two statistically independent sample values of $\mathcal{N}(0,1)$.

[18] We are using the fact that $\beta\mathcal{N}(0,a^2)=\mathcal{N}(0,\beta^2a^2)$. Our arguments here concerning the Γ's of Eqs. (2.7) can be made a little more transparent by working instead with the N's of Eqs. (2.8).

[19] See, for instance, Ref. [7], Sec. II D.